Interleukin 27R regulates CD4^{+} T cell phenotype and impacts protective immunity during *Mycobacterium tuberculosis* infection

Egidio Torrado,[1] Jeffrey J. Fountain,[1] Mingfeng Liao,[1,2,3] Michael Tighe,[1] William W. Reiley,[1] Rachel P. Lai,[4] Graeme Meintjes,[5,6] John E. Pearl,[1] Xinchun Chen,[2,3] Daniel E. Zak,[7] Ethan G. Thompson,[7] Alan Aderem,[7] Nico Ghilardi,[8] Alejandra Solache,[1] K. Kai McKinstry,[9] Tara M. Strutt,[9] Robert J. Wilkinson,[4,5,6] Susan L. Swain,[9] and Andrea M. Cooper[1]

[1]Trudeau Institute, Saranac Lake, NY 12983
[2]Guangdong Key Laboratory for Emerging Infectious Disease and [3]Shenzhen Key Laboratory of Infection and Immunity, Shenzhen Third People's Hospital, Guangdong Medical College, Shenzhen 518112, China
[4]Mill Hill Laboratory, The Francis Crick Institute, London NW7 1AA, England, UK
[5]Clinical Infectious Diseases Research Initiative, Institute of Infectious Disease and Molecular Medicine, University of Cape Town, Rondebosch 7701, Cape Town, South Africa
[6]Department of Medicine, Imperial College London, London SW7 2AZ, England, UK
[7]Center for Infectious Disease Research (formerly Seattle Biomedical Research Institute), Seattle, WA 98109
[8]Department of Immunology, Genentech, South San Francisco, CA 94080
[9]Department of Pathology, University of Massachusetts Medical School, Worcester, MA 01655

CD4^{+} T cells mediate protection against *Mycobacterium tuberculosis* (Mtb); however, the phenotype of protective T cells is undefined, thereby confounding vaccination efforts. IL–27 is highly expressed during human tuberculosis (TB), and absence of IL–27R (*Il27ra*) specifically on T cells results in increased protection. IL–27R deficiency during chronic Mtb infection does not impact antigen–specific CD4^{+} T cell number but maintains programmed death–1 (PD–1), CD69, and CD127 expression while reducing T–bet and killer cell lectin-like receptor G1 (KLRG1) expression. Furthermore, T–bet haploinsufficiency results in failure to generate KLRG1^{+}, antigen–specific CD4^{+} T cells, and in improved protection. T cells in *Il27ra*^{−/−} mice accumulate preferentially in the lung parenchyma within close proximity to Mtb, and antigen–specific CD4^{+} T cells lacking IL–27R are intrinsically more fit than intact T cells and maintain IL–2 production. Improved fitness of IL–27R–deficient T cells is not associated with increased proliferation but with decreased expression of cell death–associated markers. Therefore, during Mtb infection, IL–27R acts intrinsically on T cells to limit protection and reduce fitness, whereas the IL–27R–deficient environment alters the phenotype and location of T cells. The significant expression of IL–27 in TB and the negative influence of IL–27R on T cell function demonstrate the pathway by which this cytokine/receptor pair is detrimental in TB.

CORRESPONDENCE
Andrea M. Cooper:
acooper@trudeauinstitute.org

Abbreviations used: ART, antiretroviral therapy; IRIS, immune reconstitution inflammatory syndrome; LTB, latent TB; MFI, mean fluorescence intensity; MLN, mediastinal LN; Mtb, *Mycobacterium tuberculosis*; NMS, normal mouse serum; OD, other diseases; RBC, red blood cell; TB, tuberculosis.

Tuberculosis (TB) is a worldwide public health issue that, as a result of active intervention, is lowering in incidence (Dye et al., 2013). However, new tools are required to have any realistic chance of eliminating this disease. The required tools include improved diagnosis of active disease, improved drug therapy, and new vaccine strategies (Dye et al., 2013). To develop a protective vaccine, it is critical that we identify the constituents of protective immunity to TB. Data from AIDS patients clearly indicate a role for CD4^{+} T cells (Havlir and Barnes, 1999; Geldmacher et al., 2012), and the acute susceptibility seen in individuals lacking genes in the

The Rockefeller University Press $30.00
J. Exp. Med. 2015 Vol. 212 No. 9   1449-1463
www.jem.org/cgi/doi/10.1084/jem.20141520

1449

IFNγ macrophage activation pathway (Casanova and Abel, 2002; Filipe-Santos et al., 2006) supports the importance of CD4+ T cells producing IFNγ as an appropriate target for vaccine-induced protection. However, in humans the IFNγ response is not a reliable correlate of protection (Elias et al., 2005), and a recent vaccine targeting the induction of IFNγ-producing T cells did not demonstrate improved efficacy over BCG vaccination alone (Tameris et al., 2013). Although new concepts should be developed, it is not yet appropriate to dismiss cytokine-producing CD4+ T cells as targets for effective vaccination, particularly as we do not know what the essential components of an effective CD4+ T cell response to TB are. Critical features of the protective CD4+ T cell response depend on kinetics of recruitment to the lung as well as survival and location of the cells within the lung when they arrive (Cooper, 2009; Sakai et al., 2014). We and others discovered that mice infected with *Mycobacterium tuberculosis* (Mtb), which lacked the α subunit of the IL-27 receptor (IL-27Ra, $Il27ra^{-/-}$ mice), are able to maintain lower bacterial burdens in the lung compared with control mice (Pearl et al., 2004; Hölscher et al., 2005). Conversely, these mice exhibited increased susceptibility to disease as a result of an enhanced inflammatory response (Hölscher et al., 2005). These data suggest that IL-27 could play a regulatory role that dually limits protective function, perhaps to limit immunopathology.

IL-27 is a heterodimeric cytokine formed by the association of the subunits p28 (*Il27*) and Epstein–Barr virus–induced gene 3 (EBI3 [*Ebi3*]; Pflanz et al., 2002). Although myeloid cells are the main source of the cytokine, its receptor, composed of WSX1/TCCR (encoded by *Il27ra*) and glycoprotein 130 (gp130; encoded by *Il6st*), is expressed in multiple cells (Pflanz et al., 2004). IL-27 induces expression of the Th1 transcription factors T-bet and STAT1, resulting in up-regulation of the IL-12Rβ2 chain, thus enhancing the responsiveness of naive T cells to IL-12 (Hibbert et al., 2003; Takeda et al., 2003). However, mice deficient in *Il27ra* or *Ebi3* do not display major defects in IFNγ-mediated responses (Yoshida et al., 2001; Artis et al., 2004), suggesting that where IL-12 is not limiting, IL-27 is most likely redundant for this function. This appears to be the case during Mtb infection in $Il27ra^{-/-}$ mice, wherein the kinetics of IFNγ-producing T cell accumulation in the lungs are not impaired (Pearl et al., 2004; Hölscher et al., 2005), although antigen-specific T cells from the lungs of $Il27ra^{-/-}$ mice produce lower amounts of IFNγ on a per-cell basis (Pearl et al., 2004). Because IFNγ and IFNγ-producing T cells are thought to be required for efficient macrophage activation and containment of Mtb growth, the effects of IL-27R during TB seem counterintuitive and need to be further examined.

IL-27 acts to define the T cell phenotype in many infection models (Hunter and Kastelein, 2012), and distinct phenotypes of CD4+ T cells develop during Mtb infection in mice (Reiley et al., 2010). CD4+ T cells in the lungs of infected mice express programmed death-1 (PD-1) and killer cell lectin-like receptor G1 (KLRG1), which are not associated with functional exhaustion, but rather with distinct functional properties (Reiley et al., 2010; Sakai et al.,

2014). Indeed, PD-1+ CD4+ T cells make low levels of IFNγ and proliferate in contrast to KLRG1+ CD4+ T cells, which make high levels of IFNγ but do not proliferate (Reiley et al., 2010). Moreover, in adoptive transfer experiments, PD-1+ CD4+ T cells differentiate into KLRG1+, whereas KLRG1+ CD4+ T cells maintain their phenotype and undergo rapid contraction (Reiley et al., 2010). These data support a model wherein the PD-1+ population represents a self-renewing pool within the effector population with the potential to give rise to short-lived, KLRG1+ CD4+ T cells (Reiley et al., 2010), particularly in response to a dominant epitope (Woodworth et al., 2014). Furthermore, although CD4+ KLRG1+ cells are strong effector cytokine producers, they have recently been shown to be CXCR3− and to have limited ability to migrate to the lung parenchyma and mediate control of Mtb (Sakai et al., 2014). This limited capacity to enter the lung parenchyma and engage with infected macrophage is a critical failing as T cells, which cuff around blood vessels rather than penetrating the lesion, fail to achieve optimal bacterial control (Khader et al., 2009, 2011), and direct interaction of CD4+ T cells with Mtb-infected phagocytes is critical for the protective function of CD4+ T cells (Srivastava and Ernst, 2013). Furthermore, development of KLRG1+ antigen-specific T cells after vaccination is not associated with prolonged protection, whereas KLRG1− IL-2–producing cells are (Lindenstrøm et al., 2009). Therefore, it is clear that not all effector CD4+ T cells are equally protective, which makes it critical that we define the factors leading to the differentiation of protective rather than ineffective CD4+ T cells. This will lead to the rational design of vaccines capable of promoting T cells that can enter the lung lesions, survive within them, and thereby mediate long-term protection.

Here we found that IL-27 is expressed during active TB in humans and that the loss of IL-27 receptor (IL-27R) solely on T cells results in improved protection in mice. We found that the absence of IL-27R expression during chronic Mtb results in antigen-specific T cells, which maintain PD-1, CD69, and CD127 while reducing T-bet and KLRG1 expression and which accumulate preferentially in the parenchyma, within close proximity to Mtb antigen. Antigen-specific T cells lacking IL-27R are intrinsically more fit than intact T cells, they maintain IL-2 production, and they exhibit reduced cell death markers. Our data support the hypothesis that IL-27R activity acts both intrinsically by directly impacting the T cells and extrinsically by altering the environment and that it is the combination of these effects that results in antigen-specific T cells with reduced protective efficacy. These data have important implications for the development of novel vaccination strategies for TB.

RESULTS
Absence of IL-27R on T cells results in reduced Mtb burden in the lung
In previous studies, the absence of IL-27R in the Mtb-infected mouse model resulted in reduced bacterial burden in the lungs of gene-deficient mice (Pearl et al., 2004; Hölscher et al., 2005). The components of IL-27 have also been seen

in TB granuloma (Larousserie et al., 2004) and in TB pleural effusion (Yang et al., 2012). Therefore, we wanted to determine whether IL-27 expression was associated with active disease in humans. To do this, we reanalyzed published data wherein whole blood RNA expression profiles were assessed for a large number of adults with TB in a case-control study in HIV[+] and HIV[−] populations from South Africa and Malawi (Kaforou et al., 2013). In the South African cohort, IL-27 expression was not significantly associated with HIV status (P = 0.2), but was significantly higher in TB cases compared with latently infected individuals (latent TB [LTB]; P = 3×10^{-24}) and compared with patients with other diseases (OD; P = 2×10^{-9}; Fig. 1 A). In the Malawi cohort, IL-27 expression was generally enhanced in HIV[+] compared with HIV[−] participants (P = 4×10^{-9}), but was nevertheless higher in TB cases compared with LTB (P = 10^{-17}; Fig. 1 A), and HIV had no significant effect on the difference in IL-27 levels between TB cases and LTB (P = 0.50). Furthermore, we examined IL-27 expression in TB patients coinfected with HIV who were experiencing immune reconstitution inflammatory syndrome (IRIS) as a result of antiretroviral therapy (ART; Lai et al., 2013). In a case-control study, we found that PBMCs from IRIS cases transcribe more IL-27p28 in response to Mtb than do PBMCs from controls (Fig. 1 B, left). We also used a prospective observational study to compare the IL-27p28 response at baseline between those TB/HIV individuals who developed IRIS with those who did not. We found that those who developed IRIS had a higher level of IL-27p28 in their plasma than did those who did not develop IRIS (Fig. 1 B, right). These data support the hypothesis that IL-27 is strongly up-regulated during active TB and that it may play a role in development of IRIS. These observations support further detailed analysis of the role of IL-27 in TB.

Many studies have implicated IL-27 as a modulator of T cell differentiation; however, the receptor for this cytokine is expressed widely throughout the immune system (Pflanz et al., 2004). Therefore, it was necessary to determine whether expression of IL-27R on T cells recapitulates the phenotype in the total gene-deleted mouse. To do this, we generated mice wherein only and all T cells are IL-27R deficient using BM chimeras with TCRβδ^{−/−} mice as hosts reconstituted with either 75% TCRβδ^{−/−} and 25% Il27ra^{−/−} BM (all T cells IL-27R deficient) or 75% TCRβδ^{−/−} and 25% C57BL/6 BM (all T cells are IL-27R sufficient; Fig. 1 C). These mice were efficiently reconstituted and repopulated the T cell compartment to an equivalent degree (not depicted). Upon successful reconstitution, the mice were infected via the aerosol route with Mtb and the bacterial burden in the lung was determined. We found that the number of bacteria in the lungs of the chimeras lacking IL-27R on their T cells was significantly reduced relative to the intact chimeras (Fig. 1 C) and that the bacterial burdens were similar to those we observed for intact and Il27ra^{−/−} deficient mice (Pearl et al., 2004). These data demonstrate that IL-27R expression on T cells results in a higher bacterial burden in the lungs of Mtb-infected mice.
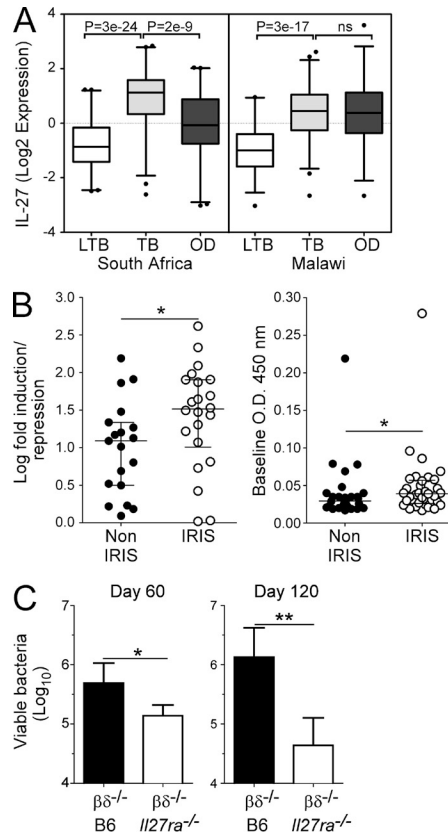

Figure 1. IL-27 is associated with active TB in humans, and resistance of *Il27ra*^{−/−} mice to Mtb locates to the T cell compartment. (A) To determine whether expression of IL-27 production is associated with active TB, microarray data were analyzed for the log2 expression (log2[1 + E − min(E)], where E represents the initial normalized data) of *IL27A* (p28 subunit). Plotted are log2 expression values after combining HIV[+] and HIV[−] cohorts and subtracting the global mean (South Africa) or residuals after modeling IL-27 expression as a function of HIV (Malawi). (B) To link excess IL-27 to IRIS, we (left) compared the Mtb-induced mRNA for *IL27A* between PBMCs from patients suffering from TB-IRIS (IRIS; n = 22) and from case controls (Non-IRIS; n = 19). The median and interquartile range are shown. (right) The level of IL-27p28 in the plasma of ART-naive HIV/TB patients who either did (IRIS; n = 33) or did not (Non-IRIS; n = 30) develop IRIS during ART. *, P < 0.05 by Mann-Whitney test. (C) TCRβδ^{−/−} mice were lethally irradiated and transplanted with a mixture of 75% TCRβδ^{−/−} plus 25% B6 (βδ^{−/−} B6) or *Il27ra*^{−/−} (βδ^{−/−} *Il27ra*^{−/−}) BM. Reconstituted mice were aerosol infected with Mtb, and bacterial burdens were determined after infection. Data are representative of two independent experiments, each with four mice per group. Error bars represent the mean ± SD. *, P < 0.05; **, P < 0.005.

The IL-27R–deficient environment impacts CD4^{+} T cell phenotype during Mtb infection

To further define the role of IL-27 in TB, we determined the impact of the IL-27R–deficient environment on the phenotype of antigen-specific T cells in the TB lesion. Using the I-A[b] ESAT-6$_{4–17}$ multimer (specific for the I-A[b] restricted epitope of the early secreted antigenic target-6 [ESAT-6]), we found that ESAT-6–specific CD4^{+} T cells expressed high levels of
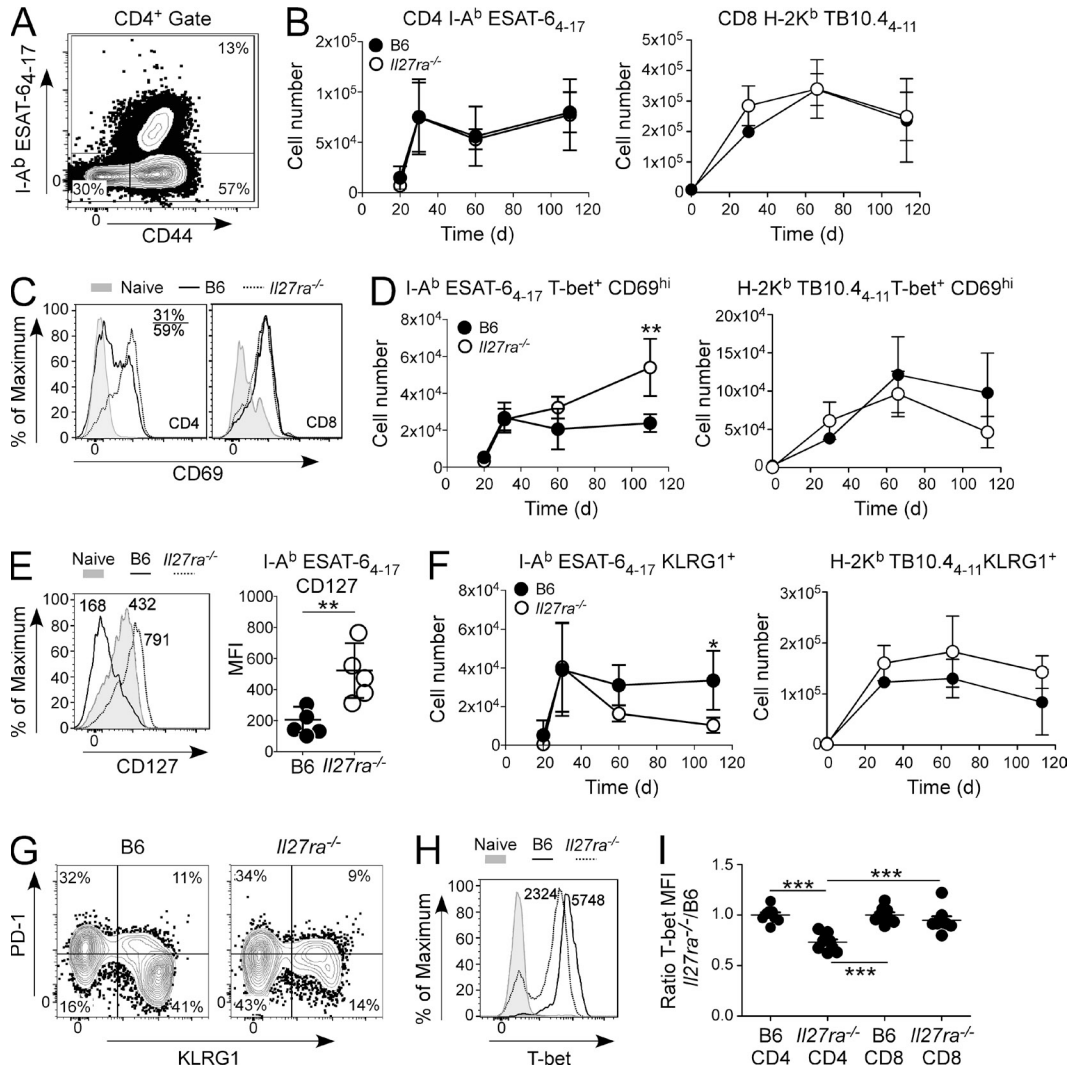
Figure 2.   IL–27R impacts the phenotype of lung CD4+ T cells during TB. (A and B) Representative FACS analysis of lung CD4+ T cells for CD44 and ESAT-6 tetramer at day 60 after infection (A) and number of I-A^b ESAT-6$_{4–17}$–specific CD4+ (left) and H-2K^b TB10.4$_{4–11}$–specific CD8+ (right) T cells in the lungs of B6 and *Il27ra$^{−/−}$* mice throughout Mtb infection (B). CD4 data are representative of three total independent experiments each with four to five mice per group. CD8 data are representative of two independent experiments with four mice per group. (C and D) Representative FACS analysis of CD69 expression by I-A^b ESAT-6$_{4–17}$–specific CD4+ and H-2K^b TB10.4$_{4–11}$–specific CD8+ T cells from B6 or *Il27ra$^{−/−}$* mice at day 110 after infection (C) and the number of CD69-expressing antigen-specific CD4 and CD8 T cells in the lungs of B6 or *Il27ra$^{−/−}$* after infection (D). CD4 data are representative of three independent experiments, each with four to five mice per group. CD8 data points represent two independent experiments with three to four mice per group. (E) Representative FACS analysis and geometric MFI of CD127 expression in I-A^b ESAT-6$_{4–17}$–specific CD4+ T cells in the lungs of B6 or IL-27R$^{−/−}$ mice at day 160 after infection. Data are representative of two independent experiments with four to five mice per group. Error bars represent the mean ± SD. (F and G) Total number (F) and representative analysis (G) of KLRG1-expressing I-A^b ESAT-6$_{4–17}$–specific CD4+ T cells in the lungs of B6 or *Il27ra$^{−/−}$* mice over time. Data are representative of a total of four independent experiments, each with four to five mice per group. H-2K^b TB10.4$_{4–11}$–specific KLRG1+ CD8+ T cells were also assessed (right). Data are representative of two independent experiments with four mice per group. (D–F) *, P < 0.05; **, P < 0.005 by Student's *t* test. (H) Representative T-bet expression in KLRG1+ or KLRG1− antigen-specific CD4+ T cells in Mtb-infected B6 mice at day 60 after infection. (I) T-bet MFI for T-bet+, antigen-specific KLRG1+ T cells from the lungs of infected B6 and *Il27ra$^{−/−}$* was determined, and the ratio of the MFI for B6 and *Il27ra$^{−/−}$* KLRG1+ T cells was compared with the mean of the B6. Data from two separate experiments (each with four to five mice per group) are combined. ***, P < 0.0001 using a one-way ANOVA followed by Dunnett's multiple comparison test. (B, D, F, and I) The mean and SD are shown.

CD44 (Fig. 2 A) and that there was an equal number of ESAT-6–specific CD4+ T cells in the lungs of both Mtb–infected B6 and *Il27ra$^{−/−}$* mice (Fig. 2 B). Antigen-specific CD8+ T cells, which bound the H–2K^b TB10.4$_{4–11}$ tetramer (Woodworth et al., 2008), also did not differ in number (Fig. 2 B). CD44+

T-bet+ CD4+ T cells, which differ in expression of CD69, differentially accumulate in mycobacterial lesions (Pearl et al., 2012), and we found that the frequency of antigen-specific, T-bet+ CD69+ T cells increased in the *Il27ra$^{−/−}$* mice during chronic infection relative to the B6 mice (Fig. 2, C and D).
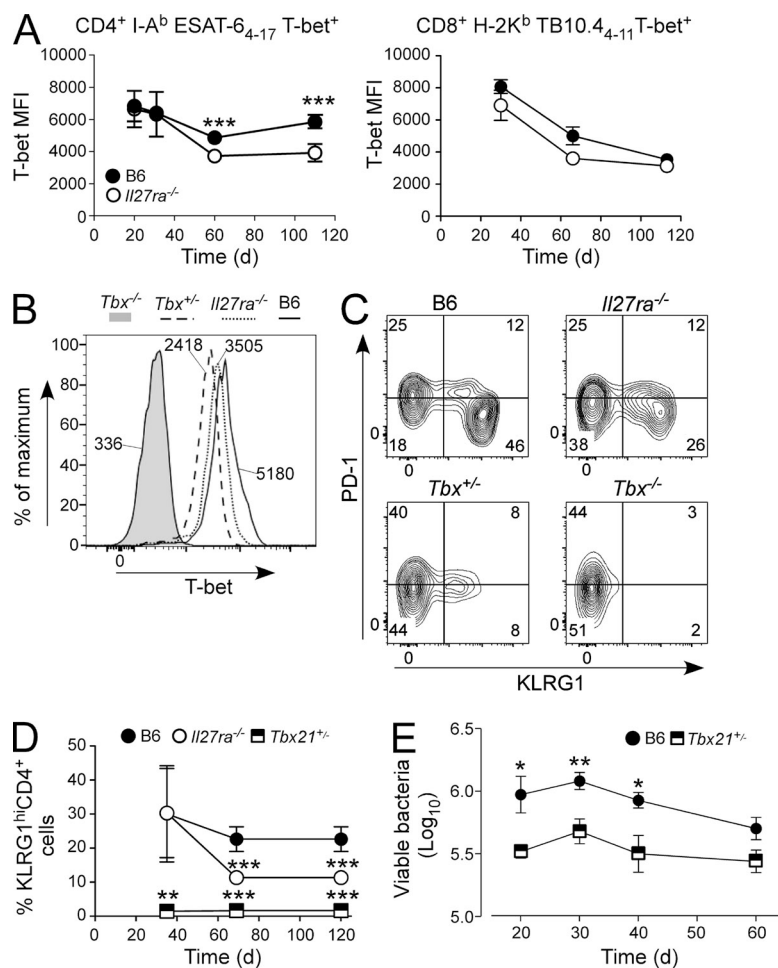
Figure 3. T–bet haploinsufficiency prevents the development of KLRG1+ CD4+ T cells and promotes improved control of Mtb. (A) FACS analysis of T-bet expression by I-A^b ESAT-6$_{4-17}$–specific CD4+ (left) and H-2K^b TB10.4$_{4-11}$–specific CD8+ (right) T cells in the lungs of B6 or *Il27ra$^{-/-}$* mice over time. CD4 data are representative of a total of five independent experiments with four to five mice per group. CD8 data are representative of two independent experiments with four mice per group. ***, P < 0.0001. (B) Representative T-bet expression in I-A^b ESAT-6$_{4-17}$–specific CD4+ T cells from the lungs of B6, *Il27ra$^{-/-}$*, T-bet–haploinsufficient (*Tbx21$^{+/-}$*), and T-bet gene–deleted (*Tbx21$^{-/-}$*) mice at day 60 after aerosol Mtb infection was determined by flow cytometry. (C) Representative FACS analysis of PD-1 and KLRG1 expression in I-A^b ESAT-6$_{4-17}$–specific CD4+ T cells from Mtb-infected B6, *Il27ra$^{-/-}$*, *Tbx21$^{-/+}$*, and *Tbx21$^{-/-}$* KLRG1^{hi} CD4+ T cells. (D) The frequency of I-A^b ESAT-6$_{4-17}$ KLRG1^{hi} CD4+ T cells in the lungs of Mtb-infected B6, *Il27ra$^{-/-}$*, or *Tbx21$^{+/-}$* mice over time. One representative experiment of two total experiments is shown, each with three to five mice per group. **, P < 0.005; ***, P < 0.0001 by ANOVA followed by Dunnett's comparison to control (B6). (E) *Tbx21$^{+/-}$* and B6 mice were infected via the aerosol route, and the number of bacteria in the lung was determined over time. Data are pooled from four independent experiments with 8–16 total mice per group. *, P < 0.05; **, P < 0.005. (A, D, and E) Error bars represent the mean ± SD.

There was no significant difference between CD69 expression in the antigen-specific CD8 T cell population under the same conditions (Fig. 2, C and D). CD127 (IL-7Rα) expression has been associated with the development of long-lived CD8 T cells (Joshi et al., 2007), and we found that antigen-specific CD4+ T cells from the lungs of Mtb-infected *Il27ra$^{-/-}$* mice express high levels of CD127 relative to the same cells from B6 mice (Fig. 2 E). CD127 expression in CD8 T cells was found to depend on KLRG1 and T-bet expression (Joshi et al., 2007), and recently, functionally distinct subsets of antigen-specific cells have been defined in the Mtb model based on expression of PD-1 and KLRG1 (Reiley et al., 2010; Sakai et al., 2014). We found that there was a significantly reduced total number and frequency of KLRG1+ antigen-specific CD4+ T cells in the chronically infected lungs of Mtb-infected *Il27ra$^{-/-}$* mice (Fig. 2, F and G). There were no significant differences in the frequency of KLRG1+ antigen-specific CD8+ T cells (Fig. 2 F). We also found that the KLRG1+ antigen-specific CD4+ T cells in the Mtb-infected lungs were the highest expressers of T-bet (Fig. 2 H). Furthermore, we found that the ratio of T-bet signal in the *Il27ra$^{-/-}$* KLRG1+ T cells to the T-bet signal in the B6 KLRG1+ T cells was significantly below 1 for the CD4+ KLRG1+ T cells, but not for the CD8+ KLRG1+ T cells (Fig. 2 I). Together, these data demonstrate

that in the chronically Mtb-infected IL-27R–intact environment, antigen-specific CD4+ T cells maintain a CD69^{lo}, T-bet^{hi}, KLRG1+, IL-7Rα^{lo} phenotype.

T-bet haploinsufficiency recapitulates the resistance of *Il27ra$^{-/-}$* mice to Mtb

We have determined that the IL-27R–deficient mice are better able to control bacterial burden over the long term and that antigen-specific CD4+ T cells in IL-27R–deficient mice have reduced levels of T-bet relative to those in B6 mice. Therefore, we wanted to determine whether the level of T-bet was an important parameter in the control of bacterial burden in Mtb infection. To do this, we determined the kinetics of T-bet expression in antigen-specific T cells and found that although high levels of T-bet were expressed by both B6 and *Il27ra$^{-/-}$* antigen-specific CD4+ T cells early in infection, T-bet expression drops over time in the *Il27ra$^{-/-}$* mice while remaining high in the B6; antigen-specific CD8 T cells in both B6 and *Il27ra$^{-/-}$* mice had high T-bet that dropped over time (Fig. 3 A). KLRG1 expression is dependent on T-bet expression (Joshi et al., 2007), so we compared KLRG1 in antigen-specific CD4+ T cells in B6, *Il27ra$^{-/-}$*, T-bet–haploinsufficient (*Tbx21$^{+/-}$*), and T-bet–deficient (*Tbx21$^{-/-}$*) mice infected with Mtb. At day 60 after challenge, antigen-specific CD4+ T cells
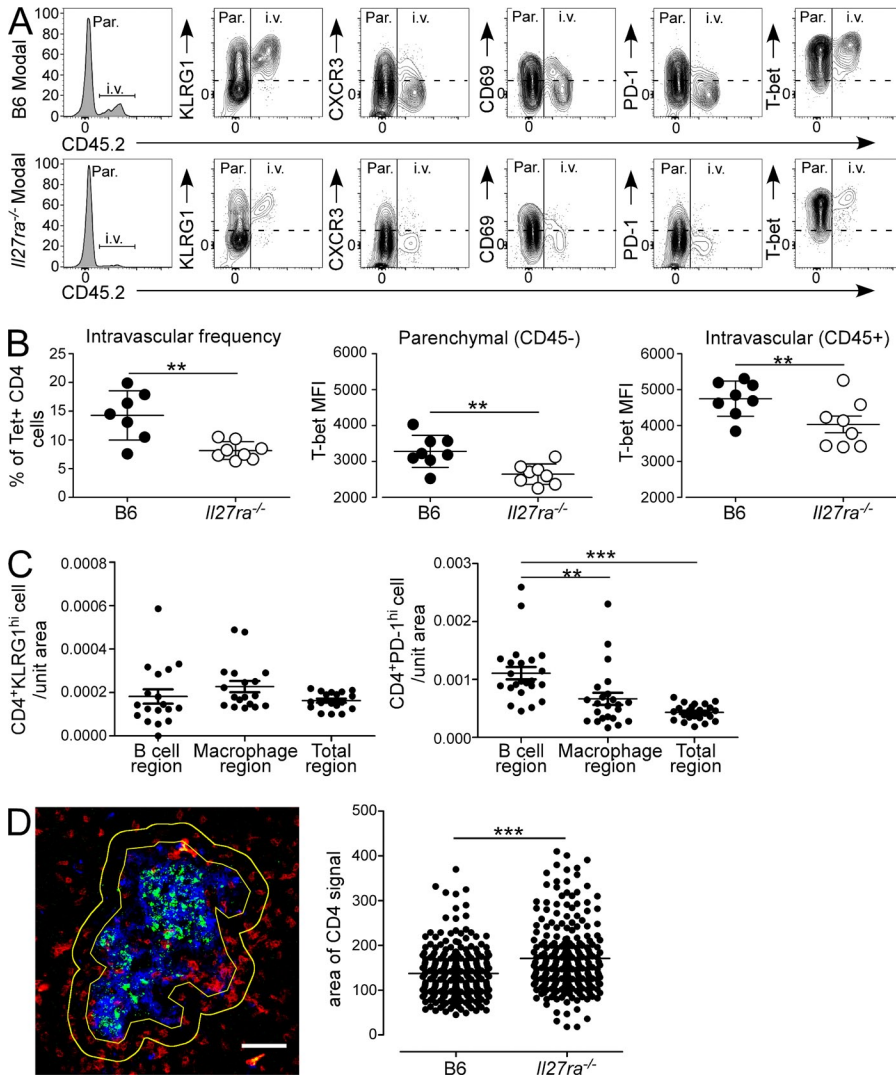
Figure 4. Absence of *Il27ra* impacts the localization of CD4+ T cells in the Mtb–infected lung. (A) To characterize parenchymal (Par) and intravascular lymphocytes, B6 (top) and *Il27ra*$^{-/-}$ (bottom) mice infected for 60 d were injected with anti–CD45-FITC antibody 3 min before harvest, and flow analysis of ESAT-6$_{1-20}$–specific T cells was performed. Representative data of two independent experiments, each with three to four mice, are shown. (B) The frequency (left) and T-bet expression levels (middle and right) of intravascular antigen-specific T cells were determined. Data represent two experiments each with three to four mice per group; mean and SD are shown. **, $P < 0.001$ by Student's *t* test. (C) B6 mice were infected for over 80 d, and the location of KLRG1+ (left) and PD-1+ (right) CD4+ T cells relative to B220+ (B cells) and CD11b+ (macrophages) was determined by immunohistochemistry. Data are pooled from two experiments, each containing four to five mice per group. **, $P < 0.001$; ***, $P < 0.0001$ by Kruskal-Wallis test with Dunn's multiple comparison test. (D, left) Frozen lung sections from B6 or *Il27ra*$^{-/-}$ mice were stained for Mtb antigen (green), CD4 (red), and CD11b (blue) and a 20-µm perimeter (yellow lines) defined in ImageJ. Bar, 50 µm. (right) The amount of CD4 T cell signal within the perimeter was determined for all detectable granulomata in two experiments combined. ***, $P < 0.001$. (C and D) Mean and SE are shown.

expressed high levels of T-bet in the B6 mice, reduced levels in the *Il27ra*$^{-/-}$ mice, and further reduced levels in the T-bet–haploinsufficient mice and had no expression in the T-bet gene–deficient mice (Fig. 3 B). Furthermore, although the B6 and *Il27ra*$^{-/-}$ mice developed an antigen-specific, KLRG1+ CD4+ T cell population, this population was greatly reduced or absent in the *Tbx21*$^{+/-}$ and *Tbx21*$^{-/-}$ mice (Fig. 3, C and D). We also found that there was a reduced bacterial burden in the *Tbx21*$^{+/-}$ mice relative to the B6 mice. Importantly, reduced bacterial burden and reduced KLRG1+ T cells were seen together and earlier in the *Tbx21*$^{+/-}$ mice than in the *Il27ra*$^{-/-}$ (Fig. 3, D and E). These data show that an intermediate level of T-bet expression correlates with improved ability to control bacterial growth and that high T-bet is associated with KLRG1 expression.

Absence of IL–27R impacts location of antigen–specific CD4+ T cell subsets in the Mtb–infection model

Recently, it has been shown that antigen-specific T-bet^{hi}, KLRG1+, CD4+ T cells preferentially accumulate in the intravascular rather than the parenchymal compartment of the

lung (Sakai et al., 2014). We therefore determined the extent to which IL-27R deficiency impacts the location of T cells within the Mtb-infected lung tissue. Using intravascular staining (Sakai et al., 2014) at day 60 of infection, we found that the antigen-specific T cells in the *Il27ra*$^{-/-}$ mice were less likely to be found in the vascular compartment compared with the intact mice (Fig. 4, A [bottom] and B [left]). As expected (Sakai et al., 2014), the majority of KLRG1+ antigen-specific CD4+ T cells were in the intravascular compartment (Fig. 4 A), whereas CXCR3-positive cells were in the parenchyma (Fig. 4 A). Importantly, the majority of the CD69+ and the PD-1+ antigen-specific CD4+ T cells were within the parenchyma (Fig. 4 A). Furthermore, although the mean fluorescence intensity (MFI) of T-bet expression was higher in the intravascular T cells compared with the parenchymal cells (Fig. 4 B, compare middle and right panels), the level of intrinsic T-bet expression in the antigen-specific T cells from the *Il27ra*$^{-/-}$ mice was lower than that in the cells from B6 mice in both populations (Fig. 4 B, middle and right). These data demonstrate that in the IL-27R–deficient Mtb-infected

mouse, antigen-specific CD4$^+$ T cells maintain an increased presence within the parenchyma relative to B6 mice.

To determine whether PD-1 and KLRG-1 are associated with T cell function once they are within the parenchyma, we determined the location of CD4$^+$ T cells relative to B220-positive (B cell follicle) areas or CD11b-positive (macrophage) areas in the lung lesions. Some KLRG1$^+$ CD4$^+$ T cells do enter the parenchyma by day 60 (Fig. 4 A), and indeed, a low frequency of KLRG1$^+$ CD4$^+$ T cells are found evenly distributed throughout the B cell and macrophage areas (Fig. 4 C). In contrast, the frequency of PD-1$^+$ CD4$^+$ T cells was higher than the KLRG1$^+$ CD4$^+$ T cells in both B cell and macrophage areas, and the PD-1$^+$ CD4$^+$ T cells preferentially associated with B cell regions relative to both the macrophage regions and the whole field (Fig. 4 C, right). CD4$^+$ T cells are more effective when they interact directly with infected macrophages (Srivastava and Ernst, 2013). We therefore wanted to determine whether the location of CD4$^+$ T cells relative to Mtb antigen within the lesional site is impacted by the absence of IL-27R activity. Using image analysis of frozen sections, we found that the amount of CD4-dependent signal (red) in close proximity (within 20 μm) to Mtb (green)-infected CD11b (blue) phagocytes was increased in the $Il27ra^{-/-}$ mice (Fig. 4 D). These data demonstrate that in the Mtb-infected IL-27R–deficient environment, CD4$^+$ T cell are better able to enter the parenchyma and interact closely with antigen-harboring myeloid cells.

IL–27R has intrinsic and extrinsic effects on CD4$^+$ T cells in Mtb infection

Our data demonstrate that T cells lacking IL-27R are better than intact T cells at controlling bacterial burden in Mtb-infected mice (Fig. 1 C). We also show that in an IL-27R–deficient environment, antigen-specific CD4$^+$ T cells have decreased KLRG1 and reduced T-bet (Fig. 2, F–I). To determine whether the expression of KLRG1 by T cells is a direct effect of IL-27R, we transferred PD-1$^+$ CD4 T cells from the lungs of Mtb-infected mice into congenically marked B6 and $Il27ra^{-/-}$ mice that were also Mtb infected. As expected, we found that the endogenous antigen-specific CD4$^+$ T cells in the lungs and mediastinal LNs (MLNs) of the $Il27ra^{-/-}$ mice had a reduced frequency of KLRG1$^+$ T cells relative to B6 T cells (Fig. 5 A, left two panels). In contrast, the transferred PD-1$^+$ T cells became KLRG1$^+$ in the lungs at the same frequency regardless of the genotype of the host (Fig. 5 A, right two panels), whereas transferred T cells in the MLNs of $Il27ra^{-/-}$ hosts exhibited a reduced frequency of KLRG1 relative to the B6 MLNs (Fig. 5 A, right two panels). A subset of the B6 hosts were treated with anti–IL-27R for 10 d after transfer, and although this had no impact on the endogenous response (Fig. 5 A, left two panels), the transferred T cells exhibited an unexpectedly increased frequency of KLRG1$^+$ in the lung (Fig. 5 A, right two panels) and spleen (not depicted) but not the MLNs (Fig. 5 A, right two panels). These data demonstrate that the impact of IL-27R activity on T cells does not fit a simple model of IL-27R directly driving KLRG1.

This is similar to the LCMV model wherein the level of inflammatory cytokine (IL-12 in this case) during priming defines the level of T-bet expression and KLRG1 expression downstream (Joshi et al., 2007).

To better define the intrinsic role of IL-27R activity on antigen-specific T cells in TB, we irradiated TCRαβ$^{-/-}$ mice and reconstituted them 50:50 with congenically marked B6 and $Il27ra^{-/-}$ BM (Fig. 5 B) to directly compare the phenotype of antigen-specific T cells with and without IL-27R under identical conditions. Using the illustrated gating scheme (Fig. 5 B), we found that although there was an equivalent frequency of $Il27ra^{-/-}$ and B6 non-CD4$^+$ lymphocytes (i.e., a ratio of 1) through day 120 of infection, there was a higher frequency of $Il27ra^{-/-}$ CD4$^+$ T cells (ratio above 1) skewing toward a predominance of $Il27ra^{-/-}$ CD4$^+$ T cells and becoming very pronounced in the antigen-specific CD4$^+$ T cell (CD4$^+$ CD44$^+$ ESAT-6$^+$) population (Fig. 5 C). In preliminary experiments, the KLRG1 and T-bet expressions were not dissimilar between the two groups of T cells (not depicted), suggesting that the development of the T-bet and KLRG1 phenotype is an extrinsic effect of the IL-27R–deficient environment. In separate chimeras, we determined that the bacterial burden in the lungs of the mice receiving 50:50 B6/$Il27ra^{-/-}$ BM was significantly reduced relative to the mice reconstituted with 100% B6 BM (Fig. 5 D). These data show that antigen-specific T cells that lack IL-27R are intrinsically more fit within the Mtb-infected lesion than intact T cells and that this increased fitness correlates with improved control of bacterial burden.

We have recently shown that a late paracrine IL-2 signal is required for CD4 T cells to enter into a long-lived state, which is associated with down-regulation of apoptotic pathways and permanent up-regulation of CD127 (McKinstry et al., 2014). In light of the high CD127 on T cells in the Mtb-infected $Il27ra^{-/-}$ mice and the increased fitness of $Il27ra^{-/-}$ T cells, we wanted to determine whether $Il27ra^{-/-}$ CD4$^+$ T cells have a differential ability to produce IL-2. Using the mixed BM chimera model, we found that there was a significantly higher frequency and number of T cells capable of producing IL-2 in response to antigen in the $Il27ra^{-/-}$ T cells relative to intact T cells (Fig. 6, A and B). In contrast, although the number of IFNγ-producing T cells was increased in the $Il27ra^{-/-}$ compartment, the frequency of IFNγ producers was not altered (Fig. 6 C). Furthermore, when naive B6 and $Il27ra^{-/-}$ TCRTg T cells were co-transferred into congenically marked Mtb-infected intact mice, the frequency of IL-2–producing $Il27ra^{-/-}$ TCRTg T cells was increased relative to the B6 TCRTg T cells, whereas the frequency of IFNγ-producing TCRTg T cells remained equivalent (Fig. 6, D and E). These data demonstrate that the absence of IL-27R on antigen-specific T cells in the Mtb infection model allows T cells to maintain an IL-2–producing phenotype.

Absence of IL–27R impacts accumulation of antigen–specific CD4$^+$ T cell subsets in the Mtb infection model

We wanted to examine the basis for the increased ability of antigen-specific T cells to accumulate in the absence of IL-27R.
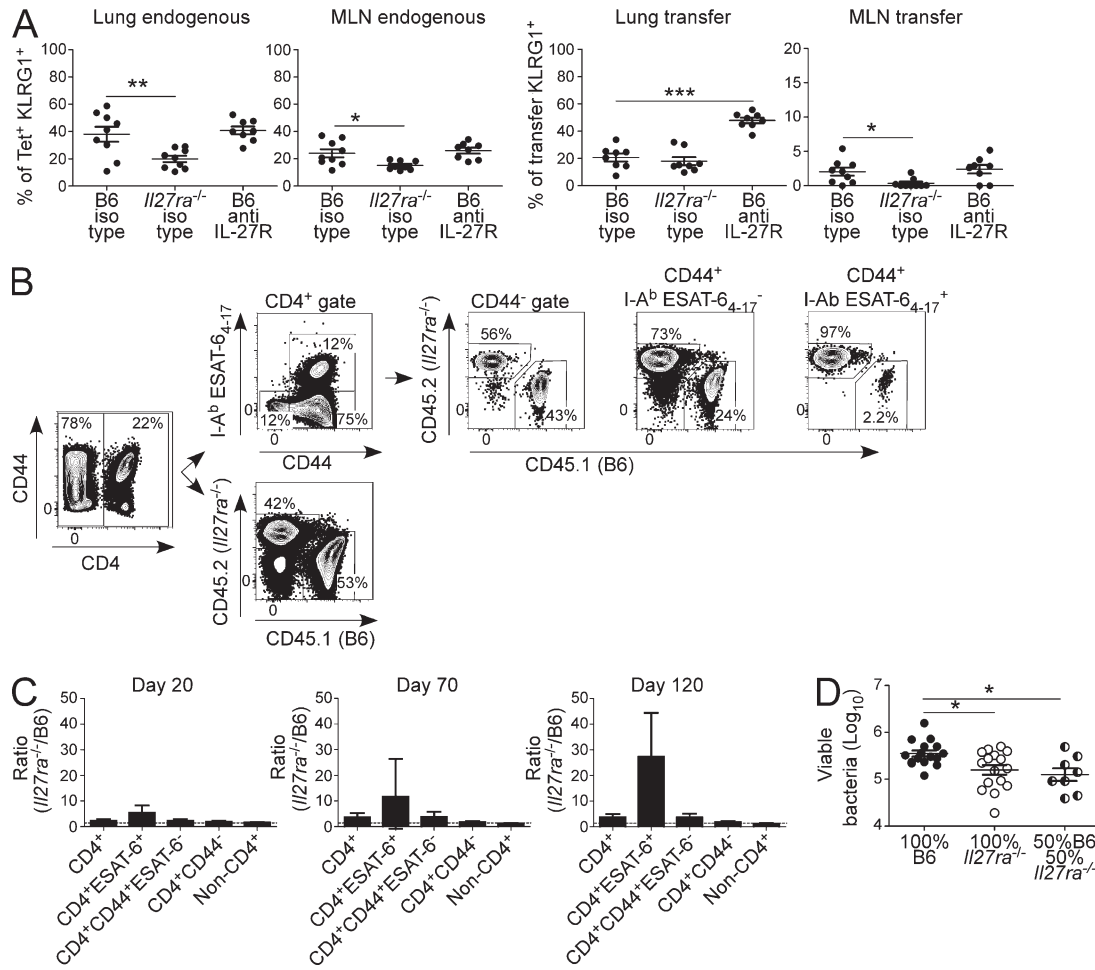
Figure 5. CD4+ T cells that lack *Il27ra* are more fit than intact T cells in the Mtb lung. (A) CD4+ PD-1+ T cells were purified from congenically marked B6 (CD45.1) mice that had been Mtb infected for 26 d and then transferred into B6 and *Il27ra*−/− mice that had been infected with Mtb 60–70 d previously. Recipient mice received isotype control or anti–IL-27R antibody for the period of the transfer (10 d). Antigen-specific endogenous (left two panels) and all transferred (right two panels) CD4+ T cells were examined for KLRG1 expression, and the impact of anti–IL-27R antibody treatment was determined in the lung and MLNs. Combined data from two experiments are shown, each with four mice per group. *, P < 0.05; **, P < 0.001; ***, P < 0.0001 by ANOVA. (B) Competitive BM chimeras were generated by transplanting BM containing equal numbers of B6.CD45.1 and *Il27ra*−/−.CD45.2 into lethally irradiated TCRβδ−/− mice that were then infected with Mtb via the aerosol route. Representative FACS analysis of the lungs of chimeric mice at day 120 after challenge shows the gating strategy. (C) The ratio of *Il27ra*−/− CD45.2 to B6-CD45.1 cells within each population in the lungs of chimeric mice after challenge was determined. Data are representative of a total of three independent experiments with four to five mice per group. (D) BM chimeras reconstituted with either 100% B6, *Il27ra*−/−, or mixed 50:50 B6 *Il27ra*−/− were infected with Mtb, and the bacterial burden at day 60 after challenge was determined. Data are from four experiments combined. *, P < 0.05 by ANOVA. (A, C, and D) Mean and SE (A and D) or mean and SD (C) are shown.

A previous study has demonstrated increased proliferation of T cells in the absence of IL-27R in the Mtb model (Hölscher et al., 2005), whereas our IL-2 (Fig. 6) and CD127 expression data (Fig. 2 E) suggest that increased survival may be important for the increased fitness of the IL-27R–deficient antigen-specific T cells (McKinstry et al., 2014). To compare proliferation in intact and *Il27ra*−/− T cells under identical conditions during Mtb infection, we measured the amount of BrdU incorporation into B6 and *Il27ra*−/− antigen-specific CD4+ T cells within mixed BM chimeras over time and found decreased incorporation of BrdU in the *Il27ra*−/− T cells (Fig. 7 A). To determine whether the impact of IL-27R deficiency on fitness occurred during priming of the antigen-specific T cells,

we performed adoptive transfers of equal and low numbers of naive TCRTg ESAT-6–specific CD4+ T cells (Reiley et al., 2008) that were either intact or lacking the *Il27ra* gene (2 × 10^4 of each genotype) into mice infected with Mtb for either 30 or 60 d (Fig. 7, B and C). Regardless of the time of transfer, *Il27ra*−/− TCRTg ESAT-6–specific CD4+ T cells outcompeted B6 TCRTg ESAT-6–specific CD4+ T cells (Fig. 7, D and E), suggesting that the improved fitness of *Il27ra*−/− cells is intrinsic and not dependent on the priming events, which differ for antigen and inflammation between days 30 and 60. Moreover, the ability of B6 TCRTg ESAT-6–specific CD4+ naive T cells to outcompete the *Il27ra*−/− TCRTg ESAT-6–specific CD4+ T cells was not likely a consequence of improved
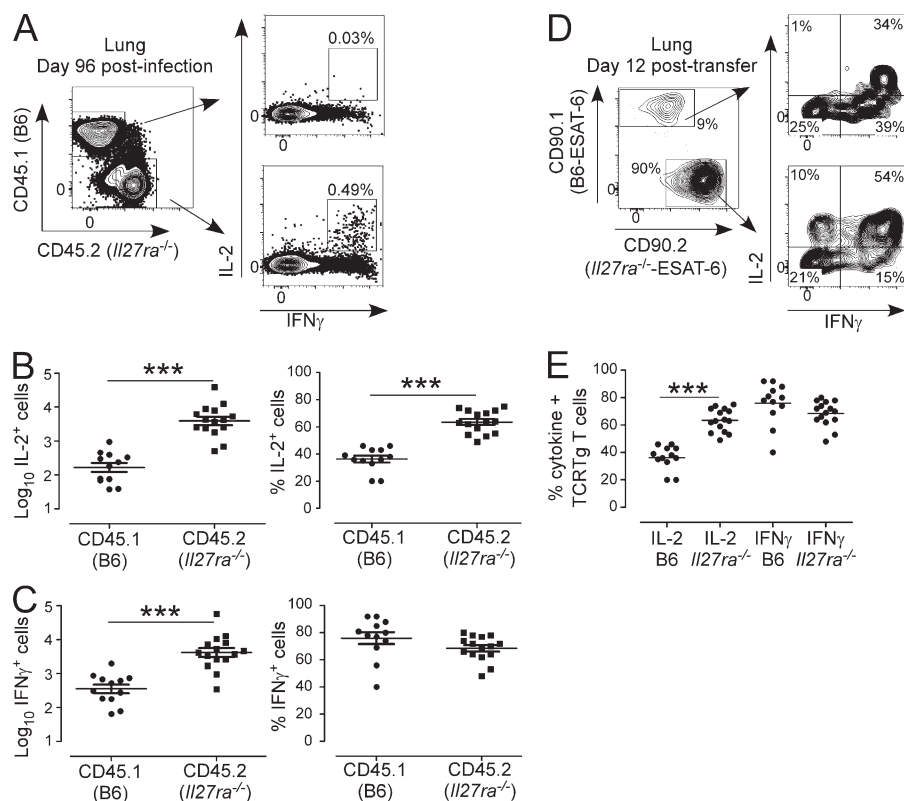
Figure 6. CD4 T cells that lack *Il27ra* are able to maintain IL–2 production during chronic Mtb infection. (A) Lung cells from Mtb-infected BM chimeric mice generated as in Fig. 5 B underwent ex vivo restimulation of with ESAT-6$_{1-20}$. (B and C) The presence of IFNγ and IL-2 in B6.CD45.1 (B6, intact) and CD45.2.IL-27R–deficient (*Il27ra$^{-/-}$*) CD4$^+$ T cells was determined by flow cytometry, and the total number and frequency of antigen-specific T cells capable of producing IL-2 (B) or IFNγ (C) in response to ESAT-6$_{1-20}$ was determined. (D and E) Naive ESAT-6$_{1-20}$–specific TCRTg CD4 T cells with (B6–ESAT-6) and without (*Il27ra$^{-/-}$*–ESAT-6) IL-27R expression were co-transferred into congenically marked Mtb-infected mice, and the lung cells were examined by flow cytometry 9 d after transfer. Panels show images of four concatenated samples (D), and the frequency of cytokine-producing TCRTg T cells was determined (E). Data show two independent experiments, each with five mice per group. (B, C, and E) Mean and SE are shown (B and C) or mean is shown (E). ***, P < 0.001 by ANOVA.

proliferation, as both genotypes incorporated similar levels of BrdU after a 24-h pulse (Fig. 7 F). These data suggest that the increased fitness of CD4$^+$ T cells lacking *Il27ra* is not a result of increased proliferative capacity.

Because *Il27ra$^{-/-}$* CD4$^+$ T cells outcompete B6 CD4$^+$ T cells while having similar proliferation profiles, we postulated that increased competitiveness was associated with differential susceptibility of these populations to cell death. To test this, we measured caspase activity in CD4$^+$ T cells from the lungs of Mtb-infected B6 and *Il27ra$^{-/-}$* mice with a pan-caspase activity detector and found that CD4$^+$ T cells from *Il27ra$^{-/-}$* mice expressed significantly less caspase activity compared with those from B6 mice at day 60 after infection (Fig. 7 G); cells with high caspase were also high expressers of Annexin (not depicted). In addition, we wanted to determine whether CD69 expression, which we have previously associated with increased ability to persist in mycobacterial lesions (Pearl et al., 2012), was associated with susceptibility of CD4$^+$ T cells to cell death. Importantly, although CD69^{hi} CD4$^+$ T cells displayed a small but significant increase in caspase activity in B6 relative to *Il27ra$^{-/-}$* mice, CD69^{lo} CD4$^+$ T cells from B6 mice had a higher caspase activity than did the CD69^{lo} CD4$^+$ T cells from the *Il27ra$^{-/-}$* mice (Fig. 7 H). These data demonstrate that CD4$^+$ effector T cells in intact mice are more likely to express markers of caspase activity than are effector T cells in *Il27ra$^{-/-}$* mice and are therefore more susceptible to cell death. Together, these data support a model wherein IL-27R signaling in CD4$^+$ T cells is detrimental to bacterial control and reduces the capacity of the T cells to maintain

IL–2 production and to accumulate effectively within the Mtb-infected lung tissue. In addition, antigen-specific T cells responding within the IL-27R–deficient environment fail to maintain high T-bet expression and the PD-1$^-$, CD69$^-$, KLRG1$^+$ T cell phenotype, which is prone to cell death and which populates the vascular rather than parenchymal areas of the lung. We suggest that the altered features of the antigen-specific effector T cells seen both as a result of intrinsic and extrinsic effects of IL-27R are responsible for their improved capacity to reduce bacterial burden relative to intact mice during Mtb infection.

DISCUSSION
Although the protective role of effector CD4$^+$ T cells in TB is recognized, the fact that we do not understand the specific function of these cells compromises rational vaccine design. We found that IL-27 is highly expressed during active TB and that loss of IL-27R specifically on T cells results in reduced Mtb burden in the mouse. In chronically Mtb-infected *Il27ra$^{-/-}$* mice, antigen-specific CD4$^+$ T cells maintain CD69, PD-1, and CD127 expression and exhibit reduced KLRG1 and T-bet relative to the same cells in intact mice. T-bet haploinsufficient mice fail to generate KLRG1$^+$ CD4$^+$ T cells and exhibit improved protection relative to intact mice, thereby supporting a negative role for high T-bet expression in TB. In *Il27ra$^{-/-}$* mice, antigen-specific CD4$^+$ T cells are better at entering the lung parenchyma and associating with antigen in Mtb-infected lesions than are CD4$^+$ T cells in intact mice. Critically, T cells lacking IL-27R exhibit improved
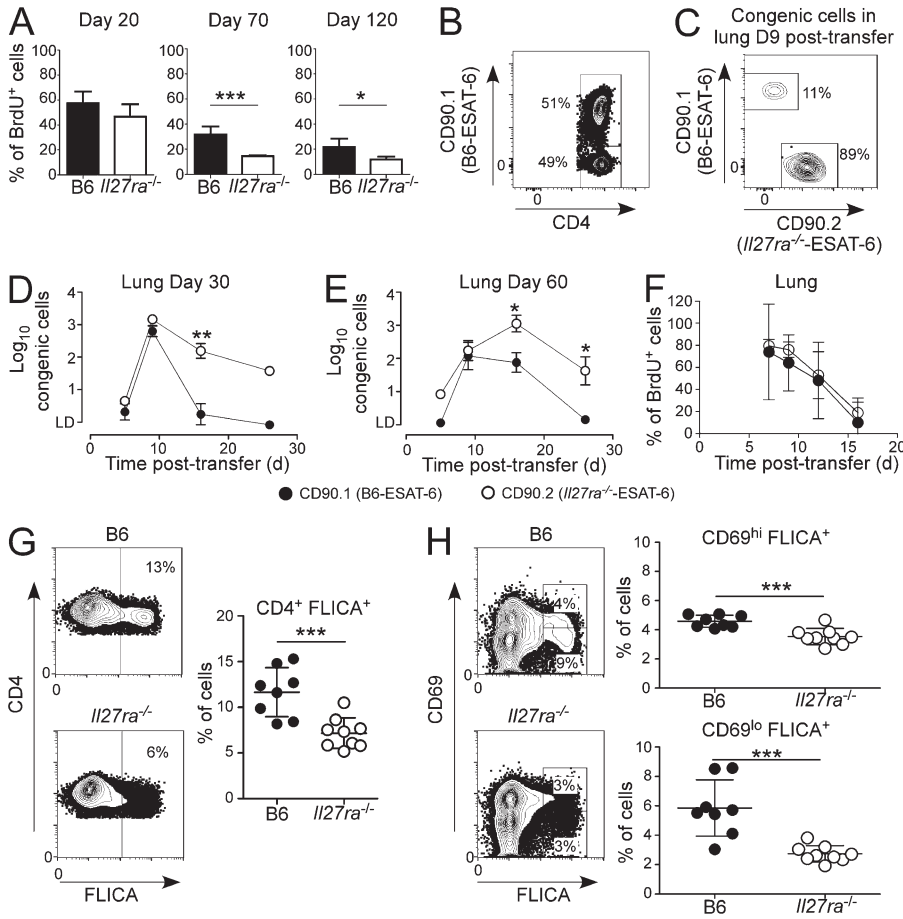
Figure 7. Absence of *Il27ra* changes the caspase activity of antigen–specific CD4 T cells. (A) BM chimeric mice were infected with Mtb and received BrdU before harvest, and the percentage of BrdU-positive I-A^b ESAT-6$_{4-17}$–specific CD4$^+$ T cells from the *Il27ra$^{-/-}$* CD45.2 or B6-CD45.1 was determined by flow. Data are representative of two independent experiments, each with four to five mice per group. *, P < 0.05; ***, P < 0.001 by Student's *t* test. (B–F) 4×10^4 naive ESAT-6$_{1-20}$–specific TCRTg CD4 T cells containing equivalent numbers of B6 ESAT-6$_{1-20}$ TCRTg and *Il27ra$^{-/-}$* ESAT-6$_{1-20}$ TCRTg cells (B) were adoptively transferred into mice infected with Mtb for 30 or 60 d. (C) Representative FACS analysis showing the relative frequency of congenically differentiated B6 and *Il27ra$^{-/-}$* ESAT-6$_{1-20}$–specific TCRTg CD4$^+$ T cells at day 9 after transfer in the lungs. (D and E) Number of B6 and *Il27ra$^{-/-}$* ESAT-6$_{1-20}$–specific TCRTg CD4$^+$ T cells in the lungs after adoptive transfer into mice infected for 30 (D) or 60 d (E) before transfer. Data are representative of nine independent experiments, each with five mice per group. (F) Incorporation of BrdU by adoptively transferred B6 and *Il27ra$^{-/-}$* ESAT-6$_{1-20}$–specific TCRTg CD4$^+$ T cells, after a 24-h pulse. Data are representative of two independent experiments, each with five mice per group. *, P < 0.05; **, P < 0.01. (G and H) Pan-caspase activity (FLICA$^+$) in lung CD4 T cells (G) or lung CD4$^+$CD69^{hi} and CD4$^+$CD69^{lo} T cells (H) from B6 or *Il27ra$^{-/-}$* mice at day 60 after infection was determined by flow. Data combine two experiments, each with four mice per group. ***, P < 0.001 by Student's *t* test. (A and D–H) Error bars represent the mean ± SD.

fitness relative to intact T cells under identical conditions, and this is associated not with increased proliferation but with improved capacity to produce IL-2 and reduced expression of markers of cell death. Together our data support a model wherein IL-27R acts directly on T cells to reduce their fitness and protective function and where the *Il27ra*-intact environment further compromises T cell function by altering their phenotype and reducing their capacity to penetrate into the infected lesion.

For effector T cells to protect, they must both be present and active at the site of infection, and this depends on their fitness and their ability to penetrate the inflamed lesion. We have previously demonstrated that expression of CD69 and increased transcription of IL-2, IL-2Rα, and IL-2Rβ are associated with increased accumulation of CD4$^+$ T cells in mycobacterial lesions (Pearl et al., 2012). Furthermore, autocrine production of IL-2 promotes up-regulation of CD127 (IL-7Rα), down-regulation of apoptosis pathways, and increased survival of CD4$^+$ T cells (McKinstry et al., 2014), whereas IL-27R deficiency results in increased IL-2 in the toxoplasma model

(Villarino et al., 2006). The increased fitness of the *Il27ra$^{-/-}$* antigen-specific CD4$^+$ T cells seen here is associated with increased IL-2 production, maintenance of CD69 and CD127 expression, and decreased expression of cell death markers. These studies, combined with our data, suggest that during chronic Mtb infection autocrine IL-2 is reduced in antigen-specific T cells by IL-27R signaling and further that the improved fitness of *Il27ra$^{-/-}$* T cells is caused by the prosurvival rather than antiproliferative activity of IL-27. Regardless of the specific pathway, it is clear that IL-27R is detrimental to effector T cell accumulation in the Mtb-induced lesion and promotes CD4$^+$ effector T cell elimination during chronic TB.

Protective T cells must be able to penetrate the infected and inflamed lesion, and determining the factors limiting this penetration is critical to vaccine design (Orme et al., 2015; Robinson et al., 2015). Both *Cxcl13* (Khader et al., 2009, 2011) and its receptor CXCR5 (Slight et al., 2013) are required for T cells to efficiently migrate into the lung parenchyma and to penetrate the infected lesion. Furthermore, T cells expressing PD-1 and CXCR3 but not KLRG1 preferentially

populate the lung parenchyma and are protective (Sakai et al., 2014; Moguche et al., 2015). Although we see a few antigen-specific KLRG1$^+$ CD4$^+$ T cells in the parenchyma by day 60 after Mtb infection, the majority of lung parenchymal, antigen-specific CD4$^+$ T cells are CD69$^+$, PD-1$^+$, and CXCR3$^+$ in both the B6 and $Il27ra^{-/-}$ mice. The major difference between these mice is that, because of the reduced frequency of KLRG1$^+$, CD69$^-$, and T-bet^{hi} CD4$^+$ T cells, the majority of antigen-specific T cells in the $Il27ra^{-/-}$ mice are within the parenchyma rather than in the vascular region. However, simply being in the parenchyma does not define protective capacity, as we know that T cells are better able to reduce bacterial number if they are in direct contact with infected phagocytes (Srivastava and Ernst, 2013). The fact that CD4$^+$ T cells in Mtb-infected $Il27ra^{-/-}$ mice are able to colocalize with Mtb antigen to a greater degree than are T cells in B6 mice suggests that part of their improved protective capacity may result from their ability to fully penetrate into the lesion; this improved penetration may reflect improved migratory capacity. Indeed, IL-27 impacts LFA-1 and intracellular adhesion molecule-1 (ICAM-1) function (Owaki et al., 2006), sphingosine-1-phosphate expression (Liao et al., 2007), and CCR5 expression (Gwyer Findlay et al., 2013), suggesting a variety of ways for IL-27 to regulate cell migration in inflamed tissue. The increased association of the PD-1$^+$ protective T cells with B cell areas that we see here may provide signals that influence migratory capacity, but this needs to be addressed further.

The tendency for vascular antigen-specific T cells to express high levels of KLRG1 and T-bet in Mtb infection (Sakai et al., 2014) supports the developing consensus that KLRG1$^+$ T cells are nonprotective in the TB mouse model. KLRG1$^+$ T cells are good at producing IFNγ but are not a self-renewing population (Reiley et al., 2010), and $Klrg1^{-/-}$ mice survive longer, with reduced bacterial burden and increased numbers of cytokine-producing T cells within the lung (Cyktor et al., 2013). KLRG1$^+$ antigen-specific T cells are less protective than PD-1$^+$ T cells in transfer models (Sakai et al., 2014; Moguche et al., 2015), and vaccine–induced KLRG1$^+$ antigen-specific T cells are less able to maintain long-term control of bacterial burden in the lung (Lindenstrøm et al., 2013; Woodworth et al., 2014). Our data further support the detrimental impact of KLRG1 expression on T cell function and show that when T-bet is limiting as a result of haploinsufficiency, antigen-specific CD4$^+$ T cells fail to develop KLRG1 expression and the bacterial burden is significantly reduced relative to when T-bet is not limiting. PD-1$^+$ antigen-specific T cells, while being poor cytokine producers, are a locally self-renewing population during Mtb infection (Reiley et al., 2010). The expression of PD-1 is also critical to survival of Mtb infection in mice (Lázár–Molnár et al., 2010; Barber et al., 2011) because of its ability to limit the pathogenic capacity of CD4$^+$ T cells (Barber et al., 2011). Recently, it has been shown that these protective, antigen-specific PD-1$^+$ T cells depend on intrinsic B cell lymphoma protein 6 (Bcl6) and inducible T cell costimulator (ICOS) expression to develop and

that they exhibit features of memory T cells (Moguche et al., 2015). In a preliminary analysis, we found that the transcriptional signal for $Icos$ was significantly, if modestly, up-regulated in CD4$^+$ T cells from $Il27ra^{-/-}$ versus intact Mtb-infected lungs ($n = 3$ samples per group, fold increase of between 1.2 and 1.5 with P = 0.02–0.007), suggesting that during chronic Mtb infection the IL-27R–deficient environment acts to drive antigen-specific CD4$^+$ T cells away from the protective self-renewing memory phenotype to the less effective KLRG1 phenotype.

IL-27R modulation of T cell function during immune-mediated responses is complex and variable and depends on where and when IL-27 is encountered (Hunter and Kastelein, 2012). Although we have clear T cell–intrinsic effects of IL-27R in the form of protection, fitness, and IL-2 expression, it does not appear that IL-27R acts directly to drive high T-bet and KLRG1 expression. We found that the IL-27R–deficient environment reduces KLRG1 expression on transferred PD-1$^+$ effector T cells in LNs but not lungs and that anti–IL-27R treatment increases KLRG1 expression in newly transferred PD-1$^+$ T cells in lung but not LN. We also found that in the absence of IL-27R, there is loss of IL-10–producing T cells (unpublished data). To mimic the loss of IL-10 seen in $Il27ra^{-/-}$ mice, we treated Mtb-infected B6 mice with anti–IL-10R (Asseman et al., 1999; Torrado et al., 2013) and found that it increased the frequency of KLRG1$^+$ CD4 T cells in the LN but not the lung (B6 isotype lung 38 ± 6 vs. B6 anti–IL-10 lung 41 ± 7, not significant; B6 isotype MLNs 28 ± 6 vs. B6 anti–IL-10 MLNs 39 ± 9, P < 0.05 by Mann-Whitney, two experiments pooled each with four mice per group). These data demonstrate that the effect of IL-27R deficiency on KLRG1 expression is time and location dependent in Mtb and may relate to relative levels of pro- and antiinflammatory cytokines both at priming and during expression of function. In malaria, IL-27R acts to repress IL-12 signaling, resulting in an increased KLRG1$^+$ population (Villegas-Mendez et al., 2013), whereas in the LCMV model, IL-12 availability during priming drives increased T-bet and KLRG1 (Joshi et al., 2007). These observations combined with the potential role of IL-10 as a regulator of IL-12 availability (Boonstra et al., 2006) and the fact that we see equivalent KLRG1 and T-bet expression in mixed chimeric mice make it clear that a simple linear model wherein IL-27R drives T-bet and subsequent KLRG1 expression cannot be proposed. Perhaps a better framework is that IL-27R signaling within the environment results in increased T-bet and KLRG1 expression and that this is mediated by, as yet, undefined factors.

IL-27 has pleiotropic effects on many cells involved in the immune response to pathogens. It acts to limit Th2 and Th17 responses by limiting GATA3 and ROR(γ)t, respectively (Lucas et al., 2003; Diveu et al., 2009); it induces IL-10 production in Th1, Th2, Th17, and Tr1 cells (Hunter and Kastelein, 2012) and T reg cells that regulate Th1-induced immunopathology (Hall et al., 2012) and promotes T cell survival in a colitis model (Kim et al., 2013). We found increased IL-17–producing antigen-specific T cells (unpublished data) and

a reduction in IL-10 CD4^{+} T cells (unpublished data), but we did not see a change in the number of forkhead box P3 (FoxP3)–expressing T cells (unpublished data) in the lungs of $Il27ra^{-/-}$ mice infected with Mtb. In the mouse malaria model, IL-27 regulates both antiparasite and immunopathologic responses (Findlay et al., 2010), as it does in Mtb (Hölscher et al., 2005), but this is not associated with loss of IL-10 or reduced T reg cells but rather caused by lost repression of IL-12–mediated signals and subsequently increased pathogenicity of the Th1 T cell response (Villegas–Mendez et al., 2013). Conversely, when $gp130$ (the coreceptor with $Il27ra$ for IL-27) is absent from macrophages and neutrophils in the Mtb model, the increased inflammation seen in Mtb-infected $Il27ra^{-/-}$ mice (Hölscher et al., 2005) is lost, without any reduction in bacterial burden (Sodenkamp et al., 2011). This publication demonstrates that the inflammatory phenotype seen in the absence of IL-27R in the Mtb model is phagocyte dependent, whereas our data demonstrate that the protective phenotype is lymphocyte dependent. Finally, other cytokines could be acting through IL-27R. Specifically, IL-27R interacts with gp130 and IL-6Rα to provide a receptor for the p28–cytokine-like factor (CLF) heterodimer, which acts on T cells and NK cells (Crabé et al., 2009). Also, the p28 subunit of IL-27 (Pflanz et al., 2004) can bind to gp130 to block the activity of IL-6, IL-27, and IL-11 (Stumhofer et al., 2010), and the balance between the cytokine subunits may be disrupted by the absence of the IL-27R. As the tools become available, further studies are required to fully differentiate the role of IL-27 on T cell function in Mtb (Hunter and Kastelein, 2012).

Together our data demonstrate that the ability of antigen-specific CD4 T cells to penetrate and persist within the Mtb-infected lung is negatively impacted by IL-27R, suggesting that vaccines that induce T cells with sustained expression of this receptor may not be protective. Rather, we should develop vaccines that promote the development of T cells able to persist within the lung environment and that can colocalize with infected phagocytes.

MATERIALS AND METHODS
Reanalysis of published microarray data. Normalized microarray data from a case-control study reporting transcriptional analysis of RNA from whole blood obtained from HIV[+] and HIV[−] individuals with LTB, active TB (TB), or OD (Kaforou et al., 2013) from South Africa and Malawi were downloaded from the Gene Expression Omnibus (series no. GSE37250) and analyzed for expression of IL-27 (p28 subunit; Illumina probe ILMN_1753758 specific for human $IL27A$). Before analysis, IL-27 expression data were processed by the transformation: $\log2(1 + E - \min(E))$, where E represents the initial normalized data. We used two-way analysis of variance to model IL-27 expression as a function of two potentially interacting factors: "HIV status" (+ or −) and "TB" (TB disease, LTB, or OD). The South Africa and Malawi cohort data were analyzed separately.

Clinical studies. Ethical approval for a case-control study of transcriptional responses in PBMCs comparing TB-IRIS and non-IRIS individuals was provided by the University of Cape Town Research Ethics Committee (REC references 337/2004 and 173/2005). Study design, patient selection criteria, and treatment regimens were as described previously (Tadokera et al., 2011, 2013). Paradoxical TB-IRIS cases were selected randomly from participants who were enrolled at the time of diagnosis with paradoxical

TB-IRIS. Non-IRIS controls were patients who were diagnosed with HIV-associated TB and thereafter started ART, but did not develop TB-IRIS within the first 3 mo of ART. Similar to cases, they were sampled at 2 wk on ART and were matched with cases based on similar CD4 count, age, sex, and duration of anti-TB treatment. PBMCs from cases and controls were stimulated with H37Rv Mtb for 6 h at a multiplicity of infection of 1. RNA was reversed transcribed and analyzed for expression of IL-27p28 using primers and probes from Applied Biosystems, (QIAGEN). The fold change from the values obtained for unstimulated controls was determined as described previously (Tadokera et al., 2013).

Ethical approval for a prospective, observational cohort study tracking HIV-TB patients receiving TB therapy before the start of ART (TB-ART2) was provided by the University of Cape Town's Faculty of Health Sciences Research Ethics Committee (REC no. 049/2009). All participants provided written informed consent. Study design, patient selection criteria, and treatment regimens were as described previously (Conesa-Botella et al., 2012; van der Plas et al., 2013). Patients were adults with serologically confirmed HIV-1 infection and a diagnosis of pulmonary or extrapulmonary TB, ART-naive at the time of recruitment. Participants were followed for 12 wk to ascertain those that developed TB-IRIS and those that did not. Whole blood was collected in sodium-heparin tubes before initiation of ART, and plasma was separated from whole blood using Ficoll-Paque (Pharmacia Biotech). Plasma was stored at −80°C until use. The first 63 patients (33 TB-IRIS and 30 non-IRIS) enrolled were selected to undergo plasma protein measurement. 10 patients (4 TB-IRIS and 6 non-IRIS) were on corticosteroid therapy at the time of collection, usually because of TB meningitis. Patients in both groups had similar clinical variables, including age, sex, CD4 count, HIV viral load, and site of Mtb infection. Patients who developed TB-IRIS had symptom onset at a median of 13 d (IQR 7–21 d) after ART initiation. The optical density of each plasma sample was determined using an IL-27p28 ELISA kit (eBioscience) according to the manufacturer's instruction.

Mice. C57BL/6, B6.129P2-$Tcrb^{tm1Mom}$ $Tcrd^{tm1Mom}$/J (TCRβδ^{−/−}), and B6.SJL-$Ptprc^a$ $Pepc^b$/BoyJ (CD45.1) mice were bred at the Trudeau Institute animal facilities from stock purchased from The Jackson Laboratory. Breeders of $Il27ra$ (TCCR/WSX1)-deficient mice ($Il27ra^{-/-}$) were provided by N. Ghilardi and F. deSauvage (Genentech), and the colony was established at Trudeau Institute. The ESAT-6 kD TCR transgenic (Tg) mice that recognize the immunodominant antigen ESAT-6$_{1-20}$ of Mtb, presented in the context of IA[b], were previously described (Reiley et al., 2008) and have been bred to be Thy1.1 ($Thy1^a$) positive and $Rag1$ negative (B6.ESAT6Tb.$Thy1^a.Rag1^{-/-}$). Thy1.2 ($Thy1^b$) TCRTg mice (B6.ESAT6 Tg.$Thy1^b.Rag^{-/-}$) mice were crossed with $Il27ra^{-/-}$ mice to generate $Il27ra^{-/-}$-ESAT6 Tg.$Thy1^b.Rag^{-/-}$ Tg mice. Both male and female mice between the ages of 6 and 12 wk old were used for experimental procedures. All procedures involving live animals were performed in accordance with the Guide for Care and Use of Laboratory Animals of the National Institutes of Health, and individual procedures were approved by the Trudeau Institute Institutional Animal Care and Use Committee.

Mtb aerosol infection and bacterial load determination. Mtb strain H37Rv was grown in Proskauer Beck medium containing 0.05% Tween-80 to mid-log phase and frozen at −70°C. Mice were infected with a low dose of bacteria (∼75 CFUs) using a Glas-Col airborne infection system as previously described (Pearl et al., 2004). At day 1 and selected time points after challenge, mice were killed by CO_2 asphyxiation, and the organs were aseptically excised and individually homogenized in saline. Organ homogenates were subsequently plated on nutrient 7H11 agar (BD Biosciences) for 3 wk at 37°C, at which point CFUs were counted.

BM chimeras and adoptive transfers. BM chimeras were generated as previously described (Torrado et al., 2013). In brief, donor BM from 6–8-wk-old mice was harvested via perfusion of the femur and tibia with cold DMEM and subsequently resuspended in lysis buffer (155 mM NH_4Cl and 10 mM $KHCO_3$) to remove red blood cells (RBCs). Cells were then washed in sterile

saline and transplanted into irradiated recipients (2×500 Rad with a 4-h interval) at 10^7/mouse. To generate chimeras that lacked *Il27ra* activity in the T cell compartment, TCRβδ$^{-/-}$ mice were lethally irradiated and transplanted with BM cells from TCRβδ$^{-/-}$ and *Il27ra*$^{-/-}$ or C57BL/6 (as control) at a ratio of 3:1, respectively. To generate competitive chimeras, TCRβδ$^{-/-}$ mice were irradiated and transplanted with a mixture of WT (CD45.1$^+$) and *Il27ra*$^{-/-}$ (CD45.2$^+$) BM at a ratio of 1:1. Recipients were kept on antibiotic-containing food for 4 wk after irradiation. 2 wk before experimental infection, BM recipients were taken off of antibiotic-containing food.

For adoptive transfer of naive CD4$^+$ T cells, cells were isolated from the spleens of ESAT6.*Thy1*^{a}.*Rag1*$^{-/-}$ (Thy1.1) or *Il27ra*$^{-/-}$-ESAT6 .*Thy1*^{b}.*Rag1*$^{-/-}$ (Thy1.2) TCRTg mice (both CD45.2) using a CD4$^+$ T cell isolation kit II (Miltenyi Biotech) according to the manufacturer's instructions. Cells were then mixed to obtain a CD4$^+$ T cell ratio of 1:1 and adoptively transferred (4×10^3 total CD4$^+$ T cells) into Mtb-infected CD45.1$^+$ mice. In some experiments, cells were labeled with 0.5 µM CFSE (Molecular Probes) for 10 min at room temperature.

For adoptive transfer of PD-1$^+$ CD4$^+$ T cells, single-cell suspensions were obtained from lung tissue, LNs, and spleens of B6.SJL-*Ptprc*^{a} *Pepc*^{b}/BoyJ (CD45.1) infected with Mtb 26 d earlier as previously described (Reiley et al., 2010). The cell suspension was panned on goat anti–mouse IgG H+L (Jackson ImmunoResearch Laboratories, Inc.)–coated T75 flasks (Falcon) for 30 min at room temperature to remove B cells and macrophages. Non-adherent cells were further enriched using the CD4$^+$ T cell isolation kit II to negatively enrich for CD4$^+$ T cells. The enriched CD4 T cells were stained with anti–PD–1–PE antibodies, followed by incubation with IMag anti-PE magnetic particles (BD). Positively selected PD-1$^+$ CD4 T cells were then counted and injected into C57BL/6 or *Il27ra*$^{-/-}$ recipient mice infected between 56 and 76 d previously. Mice receiving PD-1$^+$ T cells were also treated i.p. every 2 d with 150 µg/mouse of either an IgG2a isotype control or an anti–IL-27R antibody (clone 2918; Genentech) beginning 1 d before transfer and ending 2 d before harvest.

Lymphocyte isolation and flow cytometry. A single-cell suspension was prepared from the spleen or MLN by passing the organ through a 70-µm nylon cell strainer, followed by treatment with RBC lysis buffer. Lung cell suspensions were prepared by perfusing cold saline containing heparin through the heart, removed, and sectioned in ice-cold medium. For some experiments, mice received anti-CD45 antibody 3 min before euthanasia and lungs were not perfused (Sakai et al., 2014). Dissected lung tissue was incubated in 0.7 mg/ml collagenase IX and 30 µg/ml DNase (both from Sigma-Aldrich) at 37°C for 30 min. Digested lungs were disrupted by passage through a 70-µm nylon cell strainer, treated with RBC lysis buffer, and processed over a 40:80% Percoll (GE Healthcare) gradient. The resulting cell suspension was washed and counted. Cells were then stained with ESAT-6 or TB10.4 tetramer for 1 h at room temperature, washed, and stained with fluorochrome-conjugated antibodies for 30 min on ice. After washing, cells were processed for intracellular staining using the transcription factor buffer set (eBioscience) according to the manufacturer's instructions and stained. For intracellular cytokine detection, cells were cultured in 5 µg/ml of the cognate peptide for 1.5 h before 10 µg/ml Brefeldin A (Sigma-Aldrich) was added to the culture for 3.5 h more. Antibodies specific for CD4 (GK1.5), CD8 (53-6.7), CD44 (IM7), CD69 (H1.2F3), PD-1 (RMP1-30), KLRG1 (2F1), CD25 (3C7), CD45.1 (A20), CD45.2 (104), CD90.1 (HIS51), CD90.2 (53-2.1), CD127 (A7R34), IL-2 (JES6-5H4), IFNγ (XMG1.2), TNF (MP6-XT22), IL-17A (TC11-18H10), T-bet (4B10), and Foxp3 (FJK-16s) were from BD, BioLegend, or eBioscience. To quantify BrdU incorporation, mice were administered 0.8 mg BrdU i.p. and maintained on drinking water containing 0.8 mg/ml BrdU for 24 h before harvest. Single-cell suspensions were stained with tetramers and antibodies to surface proteins, and BrdU was detected using the BrdU Flow kit (BD). Caspase activity was assessed using the Vybrant FAM Poly Caspases Assay kit (Invitrogen) according to the manufacturer's instructions. Samples were acquired on an LSRII Special Order System flow cytometer (BD) and data analyzed using FlowJo software (Tree Star).

Histology and immunohistochemistry. The caudal lobe of each lung was inflated with 10% neutral-buffered formalin and processed routinely for light microscopy by hematoxylin and eosin stain. For immunofluorescence staining, lungs were inflated gently with OCT, frozen, and sectioned. Frozen sections were fixed in acetone/ethanol (75:25) for 10 min, washed, and blocked with 5% normal mouse serum (NMS) for 30 min. Primary antibodies (CD4 PE [BD], CD11be450 [eBioscience], rabbit anti-Mtb polyclonal [Abcam], B220 e450 [eBioscience], KLRG1 PE [SouthernBiotech], and PD-1 PE [BioLegend]) were diluted in 5% NMS and incubated with sections for 1 h. Slides were then washed and incubated with secondary antibody (anti–rabbit Alexa Fluor 594; Invitrogen) diluted in 5% NMS for 1 h and then washed. All incubations were at room temperature. Images were captured using an SP5 laser-scanning confocal microscope (Leica), and the light emissions were detected using the appropriate bandwidth settings and separate photomultiplier tubes. The data were collected as Leica image files (LIF) using LAS-AF version 2.6.0.7266 software (Leica) and converted into TIF files using Fiji software. Image analysis was performed using Fiji software (ImageJ; National Institutes of Health). Areas of interest were drawn around either B220 (B cell)- or CD11b (macrophage)-positive cellular accumulations or Mtb-positive signal (Fig. 4 D). For Fig. 4 C, the number of CD4$^+$ KLRG1$^+$ (Fig. 4 C, left) or CD4$^+$ PD-1$^+$ (Fig. 4 C, right) cells was determined and the cells per unit area calculated. For Fig. 4 D, the Mtb-positive signal area was expanded by 20 µm in all directions. The total fluorescent intensity of the CD4 channel was measured for each of these areas. This was repeated for multiple areas within a slide and also for each animal in the experiment.

Statistical analysis. Differences between the means of experimental groups were analyzed using the two-tailed Student's *t* test or ANOVA as appropriate. Differences were considered significant where $P \leq 0.05$. Inherently logarithmic data from bacterial growth was transformed for statistical analysis.

REFERENCES

Artis, D., L.M. Johnson, K. Joyce, C. Saris, A. Villarino, C.A. Hunter, and P. Scott. 2004. Cutting edge: early IL-4 production governs the requirement for IL-27-WSX-1 signaling in the development of protective Th1 cytokine responses following *Leishmania major* infection. *J. Immunol.* 172:4672–4675. http://dx.doi.org/10.4049/jimmunol.172.8.4672

Asseman, C., S. Mauze, M.W. Leach, R.L. Coffman, and F. Powrie. 1999. An essential role for interleukin 10 in the function of regulatory T cells that inhibit intestinal inflammation. *J. Exp. Med.* 190:995–1004. http://dx.doi.org/10.1084/jem.190.7.995

Barber, D.L., K.D. Mayer-Barber, C.G. Feng, A.H. Sharpe, and A. Sher. 2011. CD4 T cells promote rather than control tuberculosis in the absence of PD-1–mediated inhibition. *J. Immunol.* 186:1598–1607. http://dx.doi.org/10.4049/jimmunol.1003304

Boonstra, A., R. Rajsbaum, M. Holman, R. Marques, C. Asselin-Paturel, J.P. Pereira, E.E. Bates, S. Akira, P. Vieira, Y.J. Liu, et al. 2006. Macrophages and myeloid dendritic cells, but not plasmacytoid dendritic cells, produce IL-10 in response to MyD88- and TRIF-dependent TLR signals, and TLR-independent signals. *J. Immunol.* 177:7551–7558. http://dx.doi.org/10.4049/jimmunol.177.11.7551

Casanova, J.L., and L. Abel. 2002. Genetic dissection of immunity to mycobacteria: the human model. *Annu. Rev. Immunol.* 20:581–620. http://dx.doi.org/10.1146/annurev.immunol.20.081501.125851

Conesa-Botella, A., G. Meintjes, A.K. Coussens, H. van der Plas, R. Goliath, C. Schutz, R. Moreno-Reyes, M. Mehta, A.R. Martineau, R.J. Wilkinson, et al. 2012. Corticosteroid therapy, vitamin D status, and inflammatory cytokine profile in the HIV-tuberculosis immune reconstitution inflammatory syndrome. *Clin. Infect. Dis.* 55:1004–1011. http://dx.doi.org/10.1093/cid/cis577

Cooper, A.M. 2009. Cell-mediated immune responses in tuberculosis. *Annu. Rev. Immunol.* 27:393–422. http://dx.doi.org/10.1146/annurev.immunol.021908.132703

Crabé, S., A. Guay-Giroux, A.J. Tormo, D. Duluc, R. Lissilaa, F. Guilhot, U. Mavoungou-Bigouagou, F. Lefouili, I. Cognet, W. Ferlin, et al. 2009. The IL-27 p28 subunit binds cytokine-like factor 1 to form a cytokine regulating NK and T cell activities requiring IL-6R for signaling. *J. Immunol.* 183:7692–7702. http://dx.doi.org/10.4049/jimmunol.0901464

Cyktor, J.C., B. Carruthers, P. Stromberg, E. Flaño, H. Pircher, and J. Turner. 2013. Killer cell lectin-like receptor G1 deficiency significantly enhances survival after *Mycobacterium tuberculosis* infection. *Infect. Immun.* 81:1090–1099. http://dx.doi.org/10.1128/IAI.01199-12

Diveu, C., M.J. McGeachy, K. Boniface, J.S. Stumhofer, M. Sathe, B. Joyce-Shaikh, Y. Chen, C.M. Tato, T.K. McClanahan, R. de Waal Malefyt, et al. 2009. IL-27 blocks RORc expression to inhibit lineage commitment of Th17 cells. *J. Immunol.* 182:5748–5756. http://dx.doi.org/10.4049/jimmunol.0801162

Dye, C., P. Glaziou, K. Floyd, and M. Raviglione. 2013. Prospects for tuberculosis elimination. *Annu. Rev. Public Health.* 34:271–286. http://dx.doi.org/10.1146/annurev-publhealth-031912-114431

Elias, D., H. Akuffo, and S. Britton. 2005. PPD induced in vitro interferon gamma production is not a reliable correlate of protection against *Mycobacterium tuberculosis*. *Trans. R. Soc. Trop. Med. Hyg.* 99:363–368. http://dx.doi.org/10.1016/j.trstmh.2004.08.006

Filipe-Santos, O., J. Bustamante, A. Chapgier, G. Vogt, L. de Beaucoudrey, J. Feinberg, E. Jouanguy, S. Boisson-Dupuis, C. Fieschi, C. Picard, and J.L. Casanova. 2006. Inborn errors of IL-12/23- and IFN-γ–mediated immunity: molecular, cellular, and clinical features. *Semin. Immunol.* 18:347–361. http://dx.doi.org/10.1016/j.smim.2006.07.010

Findlay, E.G., R. Greig, J.S. Stumhofer, J.C. Hafalla, J.B. de Souza, C.J. Saris, C.A. Hunter, E.M. Riley, and K.N. Couper. 2010. Essential role for IL-27 receptor signaling in prevention of Th1-mediated immunopathology during malaria infection. *J. Immunol.* 185:2482–2492. http://dx.doi.org/10.4049/jimmunol.0904019

Geldmacher, C., A. Zumla, and M. Hoelscher. 2012. Interaction between HIV and *Mycobacterium tuberculosis*: HIV-1-induced CD4 T-cell depletion and the development of active tuberculosis. *Curr. Opin. HIV AIDS.* 7:268–275. http://dx.doi.org/10.1097/COH.0b013e3283524e32

Gwyer Findlay, E., A. Villegas-Mendez, J.B. de Souza, C.A. Inkson, T.N. Shaw, C.J. Saris, C.A. Hunter, E.M. Riley, and K.N. Couper. 2013. IL-27 receptor signaling regulates CD4+ T cell chemotactic responses during infection. *J. Immunol.* 190:4553–4561. http://dx.doi.org/10.4049/jimmunol.1202916

Hall, A.O., D.P. Beiting, C. Tato, B. John, G. Oldenhove, C.G. Lombana, G.H. Pritchard, J.S. Silver, N. Bouladoux, J.S. Stumhofer, et al. 2012. The cytokines interleukin 27 and interferon-γ promote distinct Treg cell populations required to limit infection-induced pathology. *Immunity.* 37:511–523. http://dx.doi.org/10.1016/j.immuni.2012.06.014

Havlir, D.V., and P.F. Barnes. 1999. Tuberculosis in patients with human immunodeficiency virus infection. *N. Engl. J. Med.* 340:367–373. http://dx.doi.org/10.1056/NEJM199902043400507

Hibbert, L., S. Pflanz, R. De Waal Malefyt, and R.A. Kastelein. 2003. IL-27 and IFN-α signal via Stat1 and Stat3 and induce T-Bet and IL-12Rβ2 in naive T cells. *J. Interferon Cytokine Res.* 23:513–522. http://dx.doi.org/10.1089/10799900360708632

Hölscher, C., A. Hölscher, D. Rückerl, T. Yoshimoto, H. Yoshida, T. Mak, C. Saris, and S. Ehlers. 2005. The IL-27 receptor chain WSX-1 differentially regulates antibacterial immunity and survival during experimental tuberculosis. *J. Immunol.* 174:3534–3544. http://dx.doi.org/10.4049/jimmunol.174.6.3534

Hunter, C.A., and R. Kastelein. 2012. Interleukin-27: balancing protective and pathological immunity. *Immunity.* 37:960–969. http://dx.doi.org/10.1016/j.immuni.2012.11.003

Joshi, N.S., W. Cui, A. Chandele, H.K. Lee, D.R. Urso, J. Hagman, L. Gapin, and S.M. Kaech. 2007. Inflammation directs memory precursor and short-lived effector CD8+ T cell fates via the graded expression of T-bet transcription factor. *Immunity.* 27:281–295. http://dx.doi.org/10.1016/j.immuni.2007.07.010

Kaforou, M., V.J. Wright, T. Oni, N. French, S.T. Anderson, N. Bangani, C.M. Banwell, A.J. Brent, A.C. Crampin, H.M. Dockrell, et al. 2013. Detection of tuberculosis in HIV-infected and -uninfected African adults using whole blood RNA expression signatures: a case-control study. *PLoS Med.* 10:e1001538. http://dx.doi.org/10.1371/journal.pmed.1001538

Khader, S.A., J. Rangel-Moreno, J.J. Fountain, C.A. Martino, W.W. Reiley, J.E. Pearl, G.M. Winslow, D.L. Woodland, T.D. Randall, and A.M. Cooper. 2009. In a murine tuberculosis model, the absence of homeostatic chemokines delays granuloma formation and protective immunity. *J. Immunol.* 183:8004–8014. http://dx.doi.org/10.4049/jimmunol.0901937

Khader, S.A., L. Guglani, J. Rangel-Moreno, R. Gopal, B.A. Junecko, J.J. Fountain, C. Martino, J.E. Pearl, M. Tighe, Y.Y. Lin, et al. 2011. IL-23 is required for long-term control of *Mycobacterium tuberculosis* and B cell follicle formation in the infected lung. *J. Immunol.* 187:5402–5407. http://dx.doi.org/10.4049/jimmunol.1101377

Kim, G., R. Shinnakasu, C.J. Saris, H. Cheroutre, and M. Kronenberg. 2013. A novel role for IL-27 in mediating the survival of activated mouse CD4 T lymphocytes. *J. Immunol.* 190:1510–1518. http://dx.doi.org/10.4049/jimmunol.1201017

Lai, R.P.J., J.K. Nakiwala, G. Meintjes, and R.J. Wilkinson. 2013. The immunopathogenesis of the HIV tuberculosis immune reconstitution inflammatory syndrome. *Eur. J. Immunol.* 43:1995–2002. http://dx.doi.org/10.1002/eji.201343632

Larousserie, F., S. Pflanz, A. Coulomb-L'Herminé, N. Brousse, R. Kastelein, and O. Devergne. 2004. Expression of IL-27 in human Th1-associated granulomatous diseases. *J. Pathol.* 202:164–171. http://dx.doi.org/10.1002/path.1508

Lázár-Molnár, E., B. Chen, K.A. Sweeney, E.J. Wang, W. Liu, J. Lin, S.A. Porcelli, S.C. Almo, S.G. Nathenson, and W.R. Jacobs Jr. 2010. Programmed death-1 (PD-1)–deficient mice are extraordinarily sensitive to tuberculosis. *Proc. Natl. Acad. Sci. USA.* 107:13402–13407. http://dx.doi.org/10.1073/pnas.1007394107

Liao, J.J., M.C. Huang, and E.J. Goetzl. 2007. Cutting edge: Alternative signaling of Th17 cell development by sphingosine 1-phosphate. *J. Immunol.* 178:5425–5428. http://dx.doi.org/10.4049/jimmunol.178.9.5425

Lindenstrøm, T., E.M. Agger, K.S. Korsholm, P.A. Darrah, C. Aagaard, R.A. Seder, I. Rosenkrands, and P. Andersen. 2009. Tuberculosis subunit vaccination provides long-term protective immunity characterized by multifunctional CD4 memory T cells. *J. Immunol.* 182:8047–8055. http://dx.doi.org/10.4049/jimmunol.0801592

Lindenstrøm, T., N.P. Knudsen, E.M. Agger, and P. Andersen. 2013. Control of chronic *Mycobacterium tuberculosis* infection by CD4 KLRG1⁻ IL-2–secreting central memory cells. *J. Immunol.* 190:6311–6319. http://dx.doi.org/10.4049/jimmunol.1300248

Lucas, S., N. Ghilardi, J. Li, and F.J. de Sauvage. 2003. IL-27 regulates IL-12 responsiveness of naive CD4+ T cells through Stat1-dependent and -independent mechanisms. *Proc. Natl. Acad. Sci. USA.* 100:15047–15052. http://dx.doi.org/10.1073/pnas.2536517100

McKinstry, K.K., T.M. Strutt, B. Bautista, W. Zhang, Y. Kuang, A.M. Cooper, and S.L. Swain. 2014. Effector CD4 T-cell transition to memory requires late cognate interactions that induce autocrine IL-2. *Nat. Commun.* 5:5377. http://dx.doi.org/10.1038/ncomms6377

Moguche, A.O., S. Shafiani, C. Clemons, R.P. Larson, C. Dinh, L.E. Higdon, C.J. Cambier, J.R. Sissons, A.M. Gallegos, P.J. Fink, and K.B. Urdahl. 2015. ICOS and Bcl6-dependent pathways maintain a CD4 T cell population with memory-like properties during tuberculosis. *J. Exp. Med.* 212:715–728. http://dx.doi.org/10.1084/jem.20141518

Orme, I.M., R.T. Robinson, and A.M. Cooper. 2015. The balance between protective and pathogenic immune responses in the TB-infected lung. *Nat. Immunol.* 16:57–63. http://dx.doi.org/10.1038/ni.3048

Owaki, T., M. Asakawa, F. Fukai, J. Mizuguchi, and T. Yoshimoto. 2006. IL-27 induces Th1 differentiation via p38 MAPK/T-bet- and intercellular adhesion molecule-1/LFA-1/ERK1/2-dependent pathways. *J. Immunol.* 177:7579–7587. http://dx.doi.org/10.4049/jimmunol.177.11.7579

Pearl, J.E., S.A. Khader, A. Solache, L. Gilmartin, N. Ghilardi, F. deSauvage, and A.M. Cooper. 2004. IL-27 signaling compromises control of bacterial growth in mycobacteria-infected mice. *J. Immunol.* 173:7490–7496. http://dx.doi.org/10.4049/jimmunol.173.12.7490

Pearl, J.E., E. Torrado, M. Tighe, J.J. Fountain, A. Solache, T. Strutt, S. Swain, R. Appelberg, and A.M. Cooper. 2012. Nitric oxide inhibits the accumulation of CD4+CD44hiTbet+CD69lo T cells in mycobacterial infection. *Eur. J. Immunol.* 42:3267–3279. http://dx.doi.org/10.1002/eji.201142158

Pflanz, S., J.C. Timans, J. Cheung, R. Rosales, H. Kanzler, J. Gilbert, L. Hibbert, T. Churakova, M. Travis, E. Vaisberg, et al. 2002. IL-27, a heterodimeric cytokine composed of EBI3 and p28 protein, induces proliferation of naive CD4+ T cells. *Immunity.* 16:779–790. http://dx.doi.org/10.1016/S1074-7613(02)00324-2

Pflanz, S., L. Hibbert, J. Mattson, R. Rosales, E. Vaisberg, J.F. Bazan, J.H. Phillips, T.K. McClanahan, R. de Waal Malefyt, and R.A. Kastelein. 2004. WSX-1 and glycoprotein 130 constitute a signal-transducing receptor for IL-27. *J. Immunol.* 172:2225–2231. http://dx.doi.org/10.4049/jimmunol.172.4.2225

Reiley, W.W., M.D. Calayag, S.T. Wittmer, J.L. Huntington, J.E. Pearl, J.J. Fountain, C.A. Martino, A.D. Roberts, A.M. Cooper, G.M. Winslow, and D.L. Woodland. 2008. ESAT-6-specific CD4 T cell responses to aerosol *Mycobacterium tuberculosis* infection are initiated in the mediastinal lymph nodes. *Proc. Natl. Acad. Sci. USA.* 105:10961–10966. http://dx.doi.org/10.1073/pnas.0801496105

Reiley, W.W., S. Shafiani, S.T. Wittmer, G. Tucker-Heard, J.J. Moon, M.K. Jenkins, K.B. Urdahl, G.M. Winslow, and D.L. Woodland. 2010. Distinct functions of antigen-specific CD4 T cells during murine *Mycobacterium tuberculosis* infection. *Proc. Natl. Acad. Sci. USA.* 107:19408–19413. http://dx.doi.org/10.1073/pnas.1006298107

Robinson, R.T., I.M. Orme, and A.M. Cooper. 2015. The onset of adaptive immunity in the mouse model of tuberculosis and the factors that compromise its expression. *Immunol. Rev.* 264:46–59. http://dx.doi.org/10.1111/imr.12259

Sakai, S., K.D. Kauffman, J.M. Schenkel, C.C. McBerry, K.D. Mayer-Barber, D. Masopust, and D.L. Barber. 2014. Cutting edge: control of *Mycobacterium tuberculosis* infection by a subset of lung parenchyma-homing CD4 T cells. *J. Immunol.* 192:2965–2969. http://dx.doi.org/10.4049/jimmunol.1400019

Slight, S.R., J. Rangel-Moreno, R. Gopal, Y. Lin, B.A. Fallert Junecko, S. Mehra, M. Selman, E. Becerril-Villanueva, J. Baquera-Heredia, L. Pavon, et al. 2013. CXCR5+ T helper cells mediate protective immunity against tuberculosis. *J. Clin. Invest.* 123:712–726. http://dx.doi.org/10.1172/JCI65728

Sodenkamp, J., J. Behrends, I. Förster, W. Müller, S. Ehlers, and C. Hölscher. 2011. gp130 on macrophages/granulocytes modulates inflammation during experimental tuberculosis. *Eur. J. Cell Biol.* 90:505–514. http://dx.doi.org/10.1016/j.ejcb.2010.10.010

Srivastava, S., and J.D. Ernst. 2013. Cutting edge: Direct recognition of infected cells by CD4 T cells is required for control of intracellular *Mycobacterium tuberculosis* in vivo. *J. Immunol.* 191:1016–1020. http://dx.doi.org/10.4049/jimmunol.1301236

Stumhofer, J.S., E.D. Tait, W.J. Quinn III, N. Hosken, B. Spudy, R. Goenka, C.A. Fielding, A.C. O'Hara, Y. Chen, M.L. Jones, et al. 2010. A role for IL-27p28 as an antagonist of gp130-mediated signaling. *Nat. Immunol.* 11:1119–1126. http://dx.doi.org/10.1038/ni.1957

Tadokera, R., G. Meintjes, K.H. Skolimowska, K.A. Wilkinson, K. Matthews, R. Seldon, N.N. Chegou, G. Maartens, M.X. Rangaka, K. Rebe, et al. 2011. Hypercytokinaemia accompanies HIV-tuberculosis immune reconstitution inflammatory syndrome. *Eur. Respir. J.* 37:1248–1259. http://dx.doi.org/10.1183/09031936.00091010

Tadokera, R., K.A. Wilkinson, G.A. Meintjes, K.H. Skolimowska, K. Matthews, R. Seldon, M.X. Rangaka, G. Maartens, and R.J. Wilkinson. 2013. Role of the interleukin 10 family of cytokines in patients with immune reconstitution inflammatory syndrome associated with HIV infection and tuberculosis. *J. Infect. Dis.* 207:1148–1156. http://dx.doi.org/10.1093/infdis/jit002

Takeda, A., S. Hamano, A. Yamanaka, T. Hanada, T. Ishibashi, T.W. Mak, A. Yoshimura, and H. Yoshida. 2003. Cutting edge: role of IL-27/WSX-1 signaling for induction of T-bet through activation of STAT1 during initial Th1 commitment. *J. Immunol.* 170:4886–4890. http://dx.doi.org/10.4049/jimmunol.170.10.4886

Tameris, M.D., M. Hatherill, B.S. Landry, T.J. Scriba, M.A. Snowden, S. Lockhart, J.E. Shea, J.B. McClain, G.D. Hussey, W.A. Hanekom, et al. MVA85A 020 Trial Study Team. 2013. Safety and efficacy of MVA85A, a new tuberculosis vaccine, in infants previously vaccinated with BCG: a randomised, placebo-controlled phase 2b trial. *Lancet.* 381:1021–1028. http://dx.doi.org/10.1016/S0140-6736(13)60177-4

Torrado, E., J.J. Fountain, R.T. Robinson, C.A. Martino, J.E. Pearl, J. Rangel-Moreno, M. Tighe, R. Dunn, and A.M. Cooper. 2013. Differential and site specific impact of B cells in the protective immune response to *Mycobacterium tuberculosis* in the mouse. *PLoS ONE.* 8:e61681. http://dx.doi.org/10.1371/journal.pone.0061681

van der Plas, H., G. Meintjes, C. Schutz, R. Goliath, L. Myer, D. Baatjie, R.J. Wilkinson, G. Maartens, and M. Mendelson. 2013. Complications of antiretroviral therapy initiation in hospitalised patients with HIV-associated tuberculosis. *PLoS ONE.* 8:e54145. http://dx.doi.org/10.1371/journal.pone.0054145

Villarino, A.V., J.S. Stumhofer, C.J.M. Saris, R.A. Kastelein, F.J. de Sauvage, and C.A. Hunter. 2006. IL-27 limits IL-2 production during Th1 differentiation. *J. Immunol.* 176:237–247. http://dx.doi.org/10.4049/jimmunol.176.1.237

Villegas-Mendez, A., J.B. de Souza, S.-W. Lavelle, E. Gwyer Findlay, T.N. Shaw, N. van Rooijen, C.J. Saris, C.A. Hunter, E.M. Riley, and K.N. Couper. 2013. IL-27 receptor signalling restricts the formation of pathogenic, terminally differentiated Th1 cells during malaria infection by repressing IL-12 dependent signals. *PLoS Pathog.* 9:e1003293. http://dx.doi.org/10.1371/journal.ppat.1003293

Woodworth, J.S., Y. Wu, and S.M. Behar. 2008. *Mycobacterium tuberculosis*-specific CD8+ T cells require perforin to kill target cells and provide protection in vivo. *J. Immunol.* 181:8595–8603. http://dx.doi.org/10.4049/jimmunol.181.12.8595

Woodworth, J.S., C.S. Aagaard, P.R. Hansen, J.P. Cassidy, E.M. Agger, and P. Andersen. 2014. Protective CD4 T cells targeting cryptic epitopes of *Mycobacterium tuberculosis* resist infection-driven terminal differentiation. *J. Immunol.* 192:3247–3258. http://dx.doi.org/10.4049/jimmunol.1300283

Yang, W.B., Q.L. Liang, Z.J. Ye, C.M. Niu, W.L. Ma, X.Z. Xiong, R.H. Du, Q. Zhou, J.C. Zhang, and H.Z. Shi. 2012. Cell origins and diagnostic accuracy of interleukin 27 in pleural effusions. *PLoS ONE.* 7:e40450. http://dx.doi.org/10.1371/journal.pone.0040450

Yoshida, H., S. Hamano, G. Senaldi, T. Covey, R. Faggioni, S. Mu, M. Xia, A.C. Wakeham, H. Nishina, J. Potter, et al. 2001. WSX-1 is required for the initiation of Th1 responses and resistance to *L. major* infection. *Immunity.* 15:569–578. http://dx.doi.org/10.1016/S1074-7613(01)00206-0